

1 **Large watershed flood forecasting with high resolution**

2 **distributed hydrological model**

3 Yangbo Chen^{1*}, Ji Li¹, Huanyu Wang¹, Jianming Qin¹, Liming Dong¹

4
5 ¹Department of Water Resources and Environment, Sun Yat-sen University,
6 Guangzhou 510275, China

7
8 *Correspondence to:* Yangbo Chen (eescyb@mail.sysu.edu.cn)
9

10 **Abstract.** Distributed hydrological model has been successfully used in small
11 watershed flood forecasting, but there are still challenges for the application in large
12 watershed, one of them is the model's spatial resolution effect. To cope with this
13 challenge, two efforts could be made, one is to improve the model's computation
14 efficiency in large watershed, another is implementing the model on high performance
15 supercomputer. This study sets up a physically based distributed hydrological model
16 for flood forecasting of Liujiang River Basin in south China. Terrain data DEM, soil
17 and land use are downloaded from the website freely, and the model structure with a
18 high resolution of 200m*200m grid cell is set up. The initial model parameters are
19 derived from the terrain property data, and then optimized by using the PSO algorithm,
20 the model is used to simulate 29 observed flood events. It has been found that by
21 dividing the river channels into virtual channel sections and assuming the cross
22 section shapes as trapezoid, the Liuxihe Model largely increases computation
23 efficiency while keeping good model performance, thus making it applicable in larger
24 watersheds. This study also finds that parameter uncertainty exists for physically
25 deriving model parameters, and parameter optimization could reduce this uncertainty,
26 and is highly recommended. Computation time needed for running a distributed
27 hydrological model increases exponentially at a power of 2, not linearly with the
28 increasing of model spatial resolution, and the 200m*200m model resolution is
29 proposed for modeling Liujiang River Basin flood with Liuxihe Model in this study.
30 To keep the model with an acceptable performance, minimum model spatial

31 resolution is needed. The suggested threshold model spatial resolution for modeling
32 Liujiang River Basin flood is 500m*500m grid cell, but the model spatial resolution at
33 200m*200m grid cell is recommended in this study to keep the model a better
34 performance.

35 **Key words:** watershed flood forecasting, distributed hydrological model, Liuxihe
36 Model, parameter optimization, model spatial resolution

37

38 **1 Introduction**

39 Flooding is one of the most devastating natural disasters in the world, and huge
40 damages has been caused ([Krzmm, 1992](#), [Kuniyoshi, 1992](#), [Chen, 1995](#), [EEA, 2010](#)).

41 Flood forecasting is one of the most widely used flood mitigation measurements, and
42 watershed hydrological model is the major tool for flood forecasting. Currently the
43 most popular hydrological model for watershed flood forecasting is still the so-called
44 lumped model ([Refsgaard et. al., 1996](#)), which averages the terrain property and
45 precipitation over the watershed, so do the model parameters. Hundreds of lumped
46 models have been proposed and widely used, such as the Sacramento model proposed
47 by Burnash et. al. ([1995](#)), the Tank model proposed by Sugawara et. al. ([1995](#)), the
48 Xinanjiang model proposed by Zhao ([1977](#)), and the ARNO model proposed by
49 Todini ([1996](#)), only naming a few among others. It is widely accepted that the
50 precipitation for driving the watershed hydrological processes is usually unevenly
51 distributed over the watershed, particularly for the large watershed, so the lumped
52 model could not easily forecast the watershed flooding of large watersheds.
53 Furthermore, due to the inhomogeneity of terrain property over the watershed, which
54 is true even in very small watershed, so the watershed flood forecasting could not be
55 forecasted accurately if the model parameters are averaged over the watershed. For
56 this reasons, new models are needed to improve the watershed flood forecasting
57 capability, particularly for large watershed flood forecasting.

58

59 Development of distributed hydrological model in the past decades provides the
60 potential to improve watershed flood forecasting capability. One of the most
61 important features of the distributed hydrological model is that it divides watershed
62 terrain into grid cells, which are regarded to have the same meaning of a real
63 watershed, i.e., the grid cells have their own terrain properties and precipitation. The
64 hydrological processes are calculated at both the grid cell scale and the watershed
65 scale, and the parameters used to calculate hydrological processes are also different at
66 different grid cells. This feature makes it could describe the inhomogeneity of both
67 the terrain property and precipitation over watershed. The distributed feature of the
68 distributed hydrological model is a very important feature compared to lumped model,
69 which makes it could better simulate the watershed hydrological processes at all scale,
70 small or large. The inhomogeneity of precipitation over watershed could also be well
71 described in the model, this is very helpful in modeling large watershed hydrological
72 processes, particularly in the tropical and sub-tropical regions where the flooding is
73 driven by heavy storm. For this reason, distributed hydrological model is usually
74 regarded to have the potential to better simulate or forecast the watershed flood
75 (Ambroise et. al., 1996, Chen et. al., 2016). Employing distributed hydrological
76 model for watershed food forecasting has been a new trend(Vieux et. al., 2004, Chen
77 et. al., 2012, Céline Cattoën et. al., 2016, Witold et. al., 2016, Kauffeldt et. al., 2016).

78

79 The blueprint of distributed hydrological model is regarded to be proposed by Freeze
80 and Harlan (1969), the first distributed hydrological model was the SHE model
81 proposed by Abbott et. al. (1986a, 1986b). Distributed hydrological model requires
82 different terrain property data for every grid cells to set up the model structure, so it is
83 data driven model. In the early stage of distributed hydrological modeling, this posted
84 great challenge for distributed hydrological model's application as the data was not
85 widely available and inexpensively accessible. With the development of remote
86 sensing sensors and techniques, terrain data covering global range with high
87 resolution has got readily available and could be acquired inexpensively. For example,

88 the DEM at 30m grid cell resolution with global coverage could be freely downloaded
89 (Falorni et al., 2005, Sharma et. al., 2014), which largely pushes forward the
90 development and application of the distributed hydrological models. After that, many
91 distributed hydrological models have been proposed, such as the WATERFLOOD
92 model (Kouwen, 1988), THALES model (Grayson et al., 1992), VIC model (Liang et.
93 al., 1994), DHSVM model (Wigmosta et. al., 1994), CASC2D model (Julien et. al.,
94 1995), WetSpa model (Wang et. al., 1997), GBHM model (Yang et. al., 1997), WEP-L
95 model (Jia et. al., 2001), Vflo model (Vieux et. al., 2002), tRIBS model(Vivoni et. al.,
96 2004), WEHY model (Kavvas et al., 2004), Liuxihe model (Chen et. al., 2011, 2016),
97 and more.

98

99 Distributed hydrological model derives model parameters physically from the terrain
100 property data, and is regarded not need to calibrate model parameter, so it could be
101 used in data poor or ungauged basins. This feature of distributed hydrological model
102 made it applied widely in evaluating the impacts of climate changes and urbanization
103 on hydrology(Li et. al., 2009, Seth et. al., 2001, Ott, et. al., 2004, Vanrheenen et. al.,
104 2005, Olivera et. al., 2007). But it also was found that this feature caused parameter
105 uncertainty due to the lack of experiences and references in physically deriving model
106 parameters from the terrain property, so could not be used in fields that require high
107 flood simulated accuracy, including watershed flood forecasting. It was realized that
108 parameter optimization for distributed hydrological model is also needed to improve
109 the model's performance, and a few methods for optimizing parameters of distributed
110 hydrological model have been proposed. For example, Vieux et. al. (2003) tried a
111 so-called scalar method to adjust the model parameters, and the model performance is
112 found to be improved largely. Madsen et. al. (2003) proposed an automatic
113 multi-objective parameter optimization method with SCE algorithm for SHE model,
114 which improved the model performance also. Shafii et. al. (2009) proposed a
115 multi-objective genetic algorithm for optimizing parameters of WetSpa model, the
116 improved model result is regarded to be reasonable. Xu et. al. (2012) proposed an

117 automated parameter optimization method with SCE-UA algorithm for Liuxihe Model,
118 which improved the model performance in a small watershed flood forecasting. Chen
119 et. al. (2016) proposed an automated parameter optimization method based on PSO
120 algorithm for Liuxihe Model watershed flood forecasting, and tested in two watershed,
121 one is small, one is large. The results suggested that distributed hydrological model
122 should optimize model parameters even if there is only little available hydrological
123 data, while the derived model parameters physically from the terrain property could
124 serve as an initial parameters. The above progresses in distributed hydrological
125 model's parameter optimization has matured, and will largely improve the
126 performance of distributed hydrological model, thus pushing forward the application
127 of distributed hydrological model in real-time watershed flood forecasting.

128

129 Spatial resolution is a key factor in distributed hydrological modeling. Theoretically if
130 the spatial resolution of a distributed hydrological model is higher, i.e., the grid cell
131 size is smaller, the terrain property could be described finer, and the hydrological
132 processes could be better simulated or forecasted, so the model spatial resolution
133 should be as high as possible. But on the other hand, higher model spatial resolution
134 requires higher resolution terrain property data for model setting up which may not be
135 available in some watersheds. But the most important is that distributed hydrological
136 model uses complex equations with physical meanings to calculate the hydrological
137 processes, so it needs much more computation resources than that of lumped model,
138 and the required computation resources increases exponentially with the increasing of
139 the model spatial resolution. So in modeling flood processes of a large watershed, the
140 computation time needed for running the distributed hydrological model will be huge
141 if the model spatial resolution is kept high, which may make the model application
142 impractical due to high running cost. So if distributed hydrological model is needed to
143 be applied in large watershed, a coarser resolution is the only choose, and the model's
144 capability will be impacted with less satisfactory results. This is also called the scaling
145 effect of distributed hydrological modeling. For this reason, current application for

146 watershed flood forecasting either limited to small watershed with higher resolution
147 or coarser resolution in large watershed, i.e., a trade-off between the model
148 performance and running cost.

149

150 Nowadays forecasting large watershed flooding has been in great demands as it
151 impacts peoples and their properties at large range, but due to the scale effect, current
152 distributed hydrological models employed for large watershed are at coarser
153 resolution, which lowers its capability for flood forecasting and warning. For example,
154 past application of distributed hydrological model for large watershed flood forecasting
155 are at the resolution coarser than 1km grid cell (Lohmann et. al., 1998, Vieux et. al.,
156 2004, Stisen et. al., 2008, Rwetabula et. al., 2007), the models employed in the
157 pan-European Flood Awareness System (EFAS; Bartholmes et. al., 2009, Thielen et.
158 al., 2009, 2010, Sood et. al., 2015, Kauffeldt et. al., 2016) are at 1-10km grid cell,
159 which makes the result only applicapble for flood warning.

160

161 Challenge for distributed hydrological model application in large watershed flood
162 forecasting is its need for huge computation resources, to cope with this challenge,
163 two efforts could be made. One is to improve the computation efficiency of the
164 distributed hydrological modeling in large watershed, another is implementing the
165 model on high performance supercomputer so in the cases that the users are willing to
166 pay a high computation cost, the flood forecasting of large watershed with high
167 resolution could be done. In this study, the Liuxihe Model (Chen et. al., 2011, 2016), a
168 physically based distributed hydrological model proposed for watershed flood
169 forecasting, has been tried for flood forecasting of a large watershed in southern
170 China to validate the feasibility of distributed hydrological model's application for
171 large watershed flood forecasting.

172 **2 Method and data**

173 **2.1 Liujiang River Basin**

174 The river basin studied in this paper is the Liujiang River Basin(herein after referred
175 to as LRB) in south China, which is the first order tributary of the Pearl River. LRB
176 originates from Village Lang in Guizhou Province, and drains though Guizhou
177 Province, Guangxi Zhuang Autonomous Region and Hunan Province with 72% of its
178 drainage area in Guangxi Zhuang Autonomous Region. The length of its main channel
179 is 1121 km, the total drainage area is 58270 km² that marks it a large river basin in
180 China.

181 [Fig. 1 sketch map of Liujiang River Basin\(LRB\)](#)

182 LRB is a mountainous watershed. There are high mountains in the north and
183 northwest of the watershed with high elevation, while in its south and southeast area,
184 the elevations are relatively low. This topography helps forming severe flooding in the
185 middle and downstream. The basin is in the sub-tropical monsoon climate zone with
186 an average annual precipitation of 1800 mm, and the precipitation distribution is
187 highly uneven both at spatial and temporal with 80% of its annual precipitation occurs
188 in the summer. LRB is in the center of storm zone of Zhuang Autonomous Region,
189 heavy storm was very frequent in the past. There are 59 disastrous flooding in the past
190 400 years with recording since 1488, which makes LRB the tributary with most
191 disastrous flooding among all the first order tributaries of the Pearl River. In the
192 watershed, there is no significant reservoirs to store flood runoff, so flood forecasting
193 is one of the most effective ways for the flood management.

194 **2.2 Liuxihe Model**

195 Liuxihe Model is a physically based distributed hydrological model proposed mainly
196 for watershed flood forecasting (Chen, 2009, Chen et. al., 2011, 2016). Like other
197 distributed hydrological models, Liuxihe Model divides the watershed into grid cell
198 based on the DEM of the studied watershed. To keep a reasonable model performance,
199 in the past experiences of Liuxihe Model research and application, the model

200 resolution is limited to 90m*90m or 100m*100m, but only used in small watersheds
201 (Chen, 2009, Chen et. al., 2011, 2013, 2016, Liao et. al., 2012 a, b, Xu et. al., 2012 a,
202 b). Precipitation, evaporation and runoff production are calculated at cell scale, runoff
203 routes first on cell, then along the cell to river channel, and finally to the watershed
204 outlet. As Liuxihe model is mainly used in the sub-tropical regions, so the runoff
205 production is calculated based on the saturation-excess mechanism(Zhao, 1977). The
206 runoff routing is classified as hill slope routing, river channel routing, subsurface
207 routing and underground routing. The hill slope routing is regarded as the
208 one-dimensional unsteady flow, and the kinematical wave approximation is employed
209 to do the routing. The river channel routing is also regarded as the one-dimensional
210 unsteady flow, but the diffusive wave approximation is employed to do the routing.
211 The above methods are widely used in the dominated distributed hydrological models.

212

213 What makes Liuxihe Model unique is that the river channel cross section shape is
214 assumed to be trapezoid. With this assumption, the river channel size could be
215 represented with 3 dimensions, including the bottom width, side slope and bottom
216 slope. One of the advantages with this assumption is that the river channel cross
217 section size could be estimated with remotely sensed data(Chen, et.al, 2011), so
218 Liuxihe Model could do river channel runoff routing real physically, thus making
219 Liuxihe Model a fully distributed hydrological model. As there are too many river
220 channel cross sections, and many of them are in the upstream of the watershed where
221 it is not easily accessed, so in real hydrological modeling, directly measuring the river
222 channel cross section sizes are impractical considering the high cost. For this reason,
223 most of the distributed hydrological model could not be applied in real applications,
224 or simply route the runoff with lumped methods which makes the model not a fully
225 distributed hydrological model, thus lowering the model's capability in simulating or
226 forecasting the watershed flood processes. Another advantage of this assumption is
227 that it also simplifies the runoff routing, thus improves the model's computation
228 efficiency. For this reason, even Liuxihe Model has a very high resolution, it still

229 could be used in real-time flood forecasting. This feature of Liuxihe Model in
230 estimating river channel cross section sizes makes it has the potential to be used in
231 large watershed flood forecasting.

232

233 Like other distributed hydrological model, when used in ungauged or data poor
234 watershed flood forecasting, Liuxihe Model derives model parameters physically
235 from the terrain property data. But if there is observed hydrological data, automatic
236 parameter optimization methods could be tried. But as automatic parameter
237 optimization needs thousands model runs, that makes it difficult to be used widely due
238 to huge computing source requirement, which also make it taking long time in setting
239 up the model. For this reason, a public computer cloud was set up for optimizing the
240 parameters of Liuxihe Model which employs parallel computation techniques and was
241 implemented on a supercomputer system(Chen et. al., 2013). With this development,
242 Liuxihe Model could easily optimize its model parameters.

243

244 Above advancements of Liuxihe Model in estimating river channel cross section sizes
245 with remotely sensed data, automatic parameters optimization and supercomputing
246 makes it has the potential to be used in large watershed flood forecasting, so in this
247 study, the Liuxihe model is employed to study the LRB's flood forecasting.

248 **2.3 Hydrological data**

249 There are 66 rain gauges installed in the watershed. In this study, hydrological data of
250 30 flood events has been collected, including the precipitation of the rain gauges and
251 the river discharge of Liuzhou river gauge that locates in the downstream of the
252 watershed and closes to the outlet as shown in Fig. 1 with a hourly step, brief
253 information of these flood events is listed in Table 1.

254 [Table1 Brief information of flood events with data collected in LRB](#)

255 **2.4 Terrain property data**

256 Terrain property data includes DEM, land use/cover map and soil map, which are

257 used for setting up the distributed hydrological model for flood forecasting. In this
258 study, the DEM was downloaded from the SRTM database (Falorni et al., 2005,
259 Sharma et. al., 2014), the land use type was downloaded from the USGS land use type
260 database (Loveland et. al., 1991, Loveland et. al., 2000), and the soil type was
261 downloaded from FAO soil type database (<http://www.isric.org>). The downloaded
262 DEM has a spatial resolution of 90m*90m, considering LRB is large, the running load
263 for the model with a resolution of 90m*90m may be too heavy to run in this study, so
264 the DEM is rescaled to the resolutions of 200m*200m, as shown in Fig. 2(a). The
265 downloaded land use and soil type were at 1000m*1000m resolution, so there are
266 rescaled to the same resolution of DEM, as shown in Fig. 2(b) and Fig. 2 (c)
267 respectively.

268 Fig. 2 Terrain properties of LRB

269 The highest elevation and the lowest elevation of LRB are 2124 m and 42 m
270 respectively. There are 9 land use types, including evergreen needle leaved
271 forest(18.1%), evergreen broadleaved forest(31.0%), shrubbery(32.5%), mountain and
272 alpine meadow(0.1%), slope grassland(13.7%), urban area(0.1%), river(0.2%),
273 lakes(0.3%) and cultivated land(4%).

274

275 There are 11 soil types, including Humicacrisol(0.8%), Haplic and high activitive
276 acrisol(1.5%), Ferralic cambisol(5%), Haplicluvisols(3.5%), Dystric cambisol(2.8%),
277 Calcaric regosol(45.5%), Dystric regosol(2.9%), Haplic and weak active acrisol(18%),
278 Artificial accumulated soil(1.5%), Eutricregosols and Black limestone soil(3.5%),
279 Dystric rankers(15%).

280 **3 Results**

281 **3.1 Liuxihe Model set up**

282 Considering LRB is large, so the DEM with 200m×200m resolution is adopted to set
283 up the model structure, not at the original 90m×90m resolution. The whole watershed
284 is first divided into 1469900 cells by the DEM horizontally, which were further

285 categorized into hill slope cells and river cells. By using Strahler method (Strahler,
286 1957), the river channel is divided into 3 order system as shown in Fig. 3, which
287 divides the whole cells into 1463204 hill slope cells and 6696 river cells.

288 [Fig. 3 Liuxihe Model structure set up for LRB \(200m×200m resolution\)](#)

289 To estimate the river channel sizes, 178 virtual nodes were set on the river channel
290 system, and 225 virtual channel sections were formed as shown in Figure 3. As in
291 Liuxihe Model, the shape of the virtual channel sections is assumed to be trapezoid,
292 so the cross section size is represented by three dimensions, including bottom width,
293 side slope and bottom slope. As proposed in Liuxihe Model, the bottom width is
294 estimated based on the satellite remote sensing imageries. For the side slope, it is a
295 low sensitive data, so it could be estimated based on local experiences. For the bottom
296 slope, it is calculated with the DEM along the virtual channel section.

297 **3.2 Parameter optimization**

298 In Liuxihe Model, an initial parameter set was derived first based on the terrain
299 properties, including the DEM, soil type and land use/cover type, then the parameters
300 will be optimized. In this study, for the insensitive parameter of the land use/cover
301 related parameters, which is the evaporation coefficient, the initial value is set to be
302 0.7 for all cells based on the experiences. The initial value of roughness, i.e., the
303 Manning's coefficient, which is the sensitive parameter of the land use/cover related
304 parameters, is derived from the land use/cover type based on references (Chen et.al.,
305 1995, Zhang et.al., 2006, 2007, Shen et.al., 2007, Guo et.al., 2010, Li et.al., 2013,
306 Zhang et.al., 2015), and listed in Table 2.

307 [Table 2 The initial values of land use/cover related parameters](#)

308 For the soil related parameters, including the water content at saturation condition, the
309 water content at field condition, the water content at wilting condition, hydraulic
310 conductivity at saturation condition, soil thickness and soil porosity characteristics
311 coefficient b. Based on past modeling experiences and references (Zaradny, 1993,
312 Anderson et al., 1996), a value of 2.5 is set to b for all soil type, and the water content

313 at wilting condition is set to be 30% of the water content at saturation condition. The
314 soil thickness is estimated based on local experiences and listed in Table 3 for all soil
315 types. The initial values of the water content at saturation condition, the water content
316 at field condition and hydraulic conductivity at saturation condition are estimated by
317 using the Soil Water Characteristics Hydraulic Properties Calculator (Arya et al., 1981)
318 based on soil texture, organic matter, gravel content, salinity and compaction. The
319 estimated initial values of soil-related parameters are listed in Table 3.

320 [Table 3 The initial values of soil related parameters](#)

321 In this study, PSO algorithm is employed to optimize the initial model parameters as
322 PSO algorithm has been integrated into the Liuxihe Model Cloud (Chen et. al., 2013,
323 Chen et. al., 2016). The number of particles of PSO algorithm is set to 20, while the
324 value range of inertia weight ω is set to 0.1 to 0.9, the value range of acceleration
325 coefficients C1 is set to 1.25 to 2.75, and C2 to 0.5 to 2.5, and the maximum iteration
326 is set to 50. Flood event of 20080609 is selected to optimize the parameters of Liuxihe
327 model, and Fig. 4 shows the result of the parameter optimization. Among them, Fig.
328 4(a) is the parameters evolving process, Fig. 4(b) is the changing curve of objective
329 function which is set to minimize the peak flow error, Fig.4(c) is the simulated
330 hydrograph of flood event 20080609 with the optimized parameters.

331 [Fig. 4 Parameter optimization results of Liuxihe Model for LRB with PSO algorithm](#)

332 From the results in Fig. 4, it could be found that after 14 evolutions, the parameters
333 optimization process converges to its optimal values, and the optimal parameters are
334 achieved, the simulated hydrological process of flood event that is used for parameter
335 optimization is quite good fitting the observed hydrological process, it could be said
336 that the parameter has a good optimization effect.

337

338 As mentioned above, the automatic parameter optimization of the distributed
339 hydrological model is very time consuming. In this study, even supercomputer is
340 employed with parallel computation techniques, the time used for this parameter

341 optimization is overwhelming, the total time used for achieving the above optimal
342 parameters of Liuxihe model for LRB flood forecasting is 220 hours, more than 9
343 days. Considering several runs are usually needed before achieving the final results,
344 so the parameter optimization procedure may take a few months, this run time is
345 really a good investment, but the validation results proves this is worth.

346 **3.3 Model validation**

347 The other 29 flood events were simulated by using the Liuxihe model with the above
348 optimized parameters, and the simulated hydrographs of 8 flood events are shown in
349 Fig. 5, the simulated hydrographs of 8 flood events with initial parameters are also
350 shown in Fig. 5.

351 [Fig. 5 Simulated flood events by Liuxihe Model with optimized parameters](#)

352 From the result of Fig. 5, it has been found that the simulated flood processes fits the
353 observation reasonably well, particularly the simulated peak flow is quite good, and
354 the simulated hydrological processes with optimized model parameter improved the
355 simulated hydrological processes largely. To further analyze the effect of parameter
356 optimization on model performance improvement, five evaluation indices of the
357 simulated flood events, including the Nash–Sutcliffe coefficient, the correlation
358 coefficient, the process relative error, the peak flow error and water balance
359 coefficient are calculated from the simulated results. Table 4 listed the 5 indices for
360 both the simulated results with the initial parameters and the optimized parameters.

361 [Table 4 Evaluation indices of the simulated flood events](#)

362 From Table 4, it could be seen that the five evaluation indices are quite good for the
363 simulated hydrological processes with the optimized model parameters. The average
364 peak flow error is 5% with 14% the maximum. The average Nash–Sutcliffe
365 coefficient, correlation coefficient, process relative error and water balance coefficient
366 are 0.82, 0.83, 0.22 and 0.87 respectively, that are also quite good for large river basin
367 flood simulation. Five evaluation indices of the simulated hydrological processes with
368 the optimized model parameters are also good improvements to those simulated with

369 the initial parameters, those are 0.64, 0.62, 0.37, 0.29 and 0.78. There are excellent
370 improving in all five indices, with the average increases of 0.18, 0.21 and 0.09 of the
371 average Nash–Sutcliffe coefficient, correlation coefficient and water balance
372 coefficient respectively, and the average decreases of the peak flow error and process
373 relative error are 24% and 15% respectively. So it could be concluded that the Liuxihe
374 Model set up in LRB with optimized parameters are reasonable and could be used for
375 flood forecasting of LRB. This also implies that parameter optimization of distributed
376 hydrological model could improve model performances, and it should be done when it
377 is possible.

378 **4 Discussions**

379 **4.1 Computation time vs model resolution**

380 To evaluate the spatial resolution scaling effect of distributed hydrological modeling
381 in LRB, the DEM with 90m*90m resolution is rescaled to the resolutions of
382 400m*400m, 500m*500m, 600m*600m and 1000m*1000m respectively, the land use
383 and soil type at 1000m*1000m resolution are also rescaled to the same resolutions of
384 the DEM used. Liuxihe models for LRB flood forecasting at the above resolutions are
385 then set up with the above methods, and the model structures are shown in Fig. 6.

386 [Fig. 6 Liuxihe Model structure set up for LRB with different resolution](#)

387 With different spatial resolution, the numbers of grid cells, hill slope cells and river
388 cells are different, but the river channel order are all set to 3, the numbers of virtual
389 channel nodes for 400m*400m, 500m*500m, 600m*600m and 1000m*1000m
390 resolution models are 100, 68, 46 and 33 respectively, numbers of grid cells, hill slope
391 cells and river cells with different model resolution are listed in Table 5. , the sizes of
392 every virtual cross sections are measured with the above method.

393 [Table 5 Grid cell numbers with different model spatial resolution](#)

394 From Table 5, it could be seen, number of grid cells of the model with 200m*200m
395 resolution is 4 times of that with 400m*400m resolution, 6.25 times of that with
396 500m*500m resolution, 9 times of that with 600m*600m resolution, and 25 times of

397 that with 1000m*1000m resolution, it increases at an approximate exponential of
398 power 2, not linearly with the model resolution.

399

400 Parameters of the models with 400m*400m, 500m*500m, 600m*600m and
401 1000m*1000m resolutions are optimized with PSO algorithm by using the same flood
402 event data, and listed in Table 6. From the results it could be seen that some
403 parameters are significantly different with resolution variation, but some changes little,
404 this implies that the model parameters are resolution-dependent.

405 [Table 6 Optimized parameters with different model spatial resolution](#)

406 Computation times required for parameter optimization are quite different. For the
407 model with 200m*200m resolution, the time for parameter optimization is 220 hours,
408 while that for models with 400m*400m, 500m*500m, 600m*600m and
409 1000m*1000m resolutions are 80, 55, 35 and 12 hours respectively. The times needed
410 for parameter optimization of the model at 200m*200m resolution is 2.75 times of
411 that for 400m*400m resolution model, 4 times of that for 500m*500m resolution
412 model, 6.3 times of that for 600m*600m resolution model, and 18.3 times of that for
413 1000m*1000m resolution model respectively. Considering the time needed for model
414 run, the 200m*200m model resolution is regarded as appropriate for LRB.

415 **5.2 Model performance vs model resolution**

416 The other 29 flood events are also simulated with the models at 400m*400m
417 resolution, 500m*500m resolution, 600m*600m resolution, and 1000m*1000m
418 resolution. Simulated hydrograph of 5 flood events, including 2 big, 2 medium and
419 one small ones are shown in Fig. 7.

420 [Fig. 7 Simulated results with different model resolutions](#)

421 From the results it could be seen that the simulated hydrological processes with 5
422 different spatial resolutions are quite different. The result simulated with
423 1000m*1000m resolution is not so good, although the flood shapes are simulated well,

424 but the peak flow are much lower than that of the observation, so the result is not
425 acceptable, and could not be recommended. The result simulated with 600m*600m
426 resolution is better than that of 1000m*1000m resolution, but there is still big peak
427 flow error, so the result with 600m*600m resolution is also not recommended. The
428 result simulated with 500m*500m resolution model is a big improvement to those
429 simulated with 600m*600m resolution and 1000m*1000m resolution model, the flood
430 shapes are more similar to the observation, and the peak flow is also get closer to the
431 observation, so it could be recommended for flood forecasting if the spatial resolution
432 could not be much finer. The result simulated with 400m*400m resolution has some
433 improvements to that of 500m*500m resolution, but it is not significant, so it is not
434 recommended to replace that at 500m*500m resolution. The result simulated with
435 200m*200m resolution model is a big improvement to those simulated with
436 400m*400m resolution and 500m*500m resolution model, the flood shapes fits the
437 observation much better, and the peak flows are much closer to the observation also, it
438 is a good simulation result and could be recommended for flood forecasting of LRB.
439 As the results are good enough so there is no need to further explore the finer model
440 resolution.

441 **5 Conclusions**

442 By employing Liuxihe Model, a physically based distributed hydrological model, this
443 study sets up a distributed hydrological model for the flood forecasting of Liujiang
444 River Basin in southern China that could be regarded as a large watershed. Terrain
445 data including DEM, soil type and land use type are downloaded from the website
446 freely, and the model structure with a high resolution of 200m*200m grid cell is set
447 up, which divides the whole watershed into 1469900 grid cells that is further divided
448 into 1463204 hill slope cells and 6696 river cells. The initial model parameters are
449 derived from the terrain property data, and then optimized by using the PSO algorithm
450 with one observed flood event, which improves the model performance largely. 29
451 observed flood events are simulated by using the model with optimized parameters,
452 the results are analyzed, and the model scaling effects are studied. Based on these

453 studies, following conclusions are suggested.

454

455 1. In Liuxihe Model, the river channels are divided into virtual channel sections, and
456 the cross section shapes are assumed to be trapezoid and the size is the same within
457 the virtual channel section. The size of the virtual channel section is simplified to
458 three indices, including bottom width, side slope and bottom slope, those are
459 estimated by using remote sensing imageries. This method not only makes the
460 distributed model application practical, but also simplifies the river channel routing
461 method. This significantly increases the model computation efficiency, and makes it
462 could be used in larger watersheds. Results in this study shows the model setting up
463 with this method has a reasonable performance, i.e., this simplification has not
464 sacrificed the model's flood simulation accuracy significantly, so this simplification
465 could be used in large watershed distributed hydrological modelling, including
466 Liuxihe model and other models.

467

468 2. Uncertainty exists for physically derived model parameters. Parameter optimization
469 could reduce parameter uncertainty, and is highly recommended to do so when there
470 is some observed hydrological data. In this study, the simulated hydrograph with
471 optimized model parameters is more fitting the observed hydrograph in shape than
472 that simulated with initial model parameters, the 5 evaluation indices are improved
473 also. The average increases of Nash–Sutcliffe coefficient, correlation coefficient and
474 water balance coefficient are 0.18, 0.21 and 0.09 respectively, the average decreases
475 of the peak flow error and process relative error are 24% and 15% respectively, this
476 implies that the model performance is improved significantly with parameter
477 optimization.

478

479 3. Computation time needed for running a distributed hydrological model increases
480 exponentially at an approximate power of 2, not linearly with the increasing of model
481 spatial resolution. In this study, the computation time required for parameter

482 optimization for the model with 200m*200m resolution is 220 hours, that is 4 times of
483 that of the model at 500m*500m and 18.3 times of that of the model at 1000m*1000m
484 resolution respectively. Based on the Liuxihe Model cloud system implemented on the
485 high performance supercomputer, the 200m*200m model resolution is the highest
486 resolution that could be fulfilled in modeling Liujiang River Basin flooding with
487 Liuxihe Model considering the computation cost. This also means that if the user
488 could pay high computation cost, then larger watershed could also be modelled with
489 Liuxihe Model by implemented the Liuxihe Model cloud system on a much more
490 advanced high performance supercomputer, this could be easily done nowadays if the
491 user thinks this investment is a worth doing.

492

493 4. In forecasting watershed flood by using distributed hydrological model, minimum
494 model spatial resolution needs to be maintained to keeping the model an acceptable
495 performance. Usually if the model spatial resolution increases, i.e., the grid cell gets
496 smaller, the model performance is better, but this will increase the run time
497 significantly, so there is a threshold model spatial resolution to keep the model
498 performance reasonable while keep the model run at the least time. In this study, the
499 threshold model spatial resolution is at 500m*500m grid cell, but the resolution at
500 200m*200m grid cell is recommended by trading-off between the computation cost
501 and the model performance. This conclusion may be different in different watersheds
502 for Liuxihe Model, or even different in the same watershed for different models.

503

504 5. Terrain data downloaded freely from the website derived the river channel system
505 that is very similar to the natural river channel system after it is rescaled from its
506 original spatial resolution of 90m*90m to 200m*200m, 500m*500m and
507 1000m*1000m, but the higher resolution DEM describes the river channel more in
508 details. This means that the freely downloaded DEM could be used to set up the
509 Liuxihe Model for Liujiang River Basin flood forecasting.

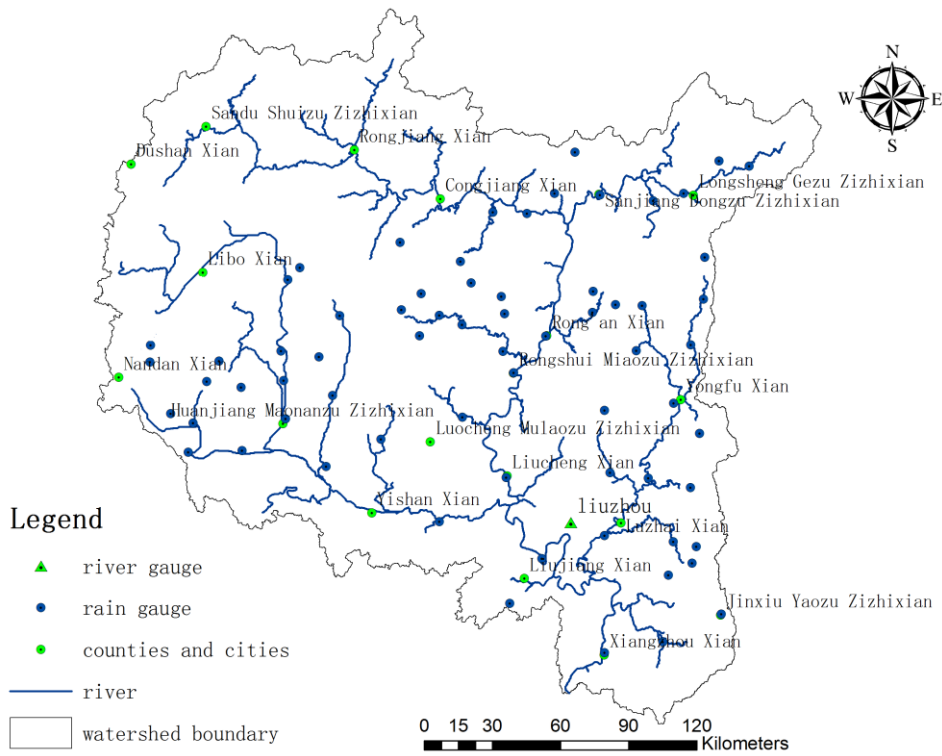
510 ***Acknowledgements:*** This study is supported by the Special Research Grant for the
511 Water Resources Industry (funding no. 201301070), the National Science Foundation
512 of China (funding no. 50479033), and the Basic Research Grant for Universities of
513 the Ministry of Education of China (funding no. 13lgjc01).

514

515

516

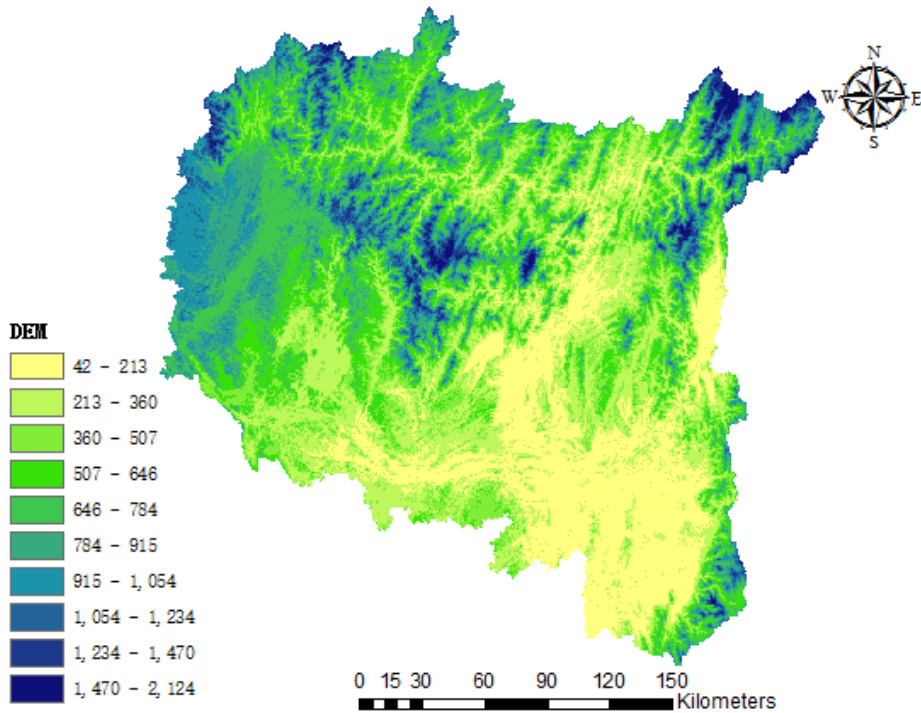
517 **Figures**



518

519

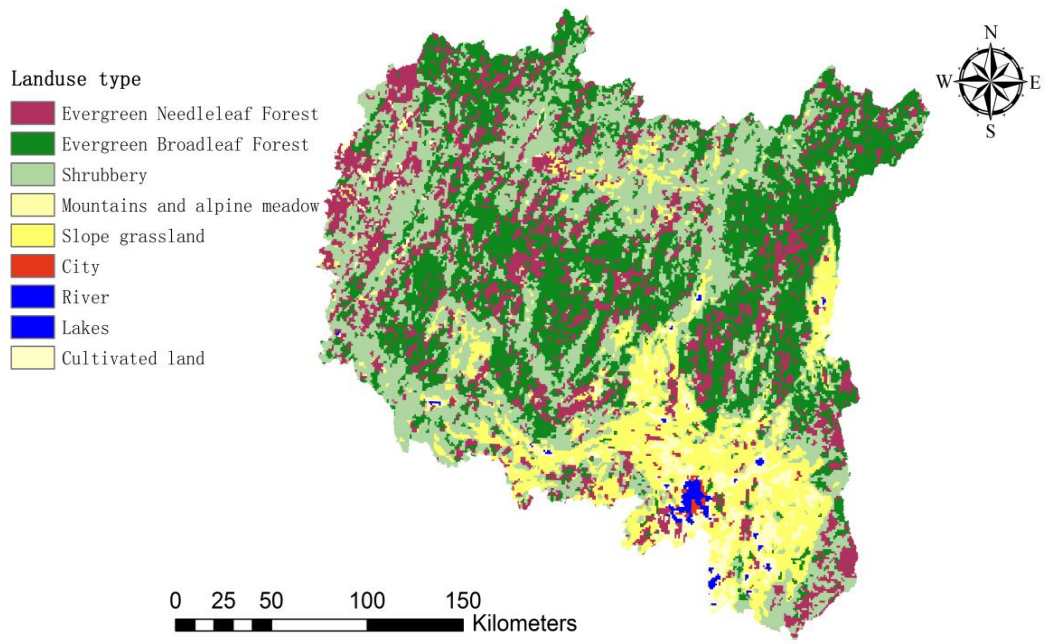
Fig. 1 sketch map of Liujiang River Basin



520

521

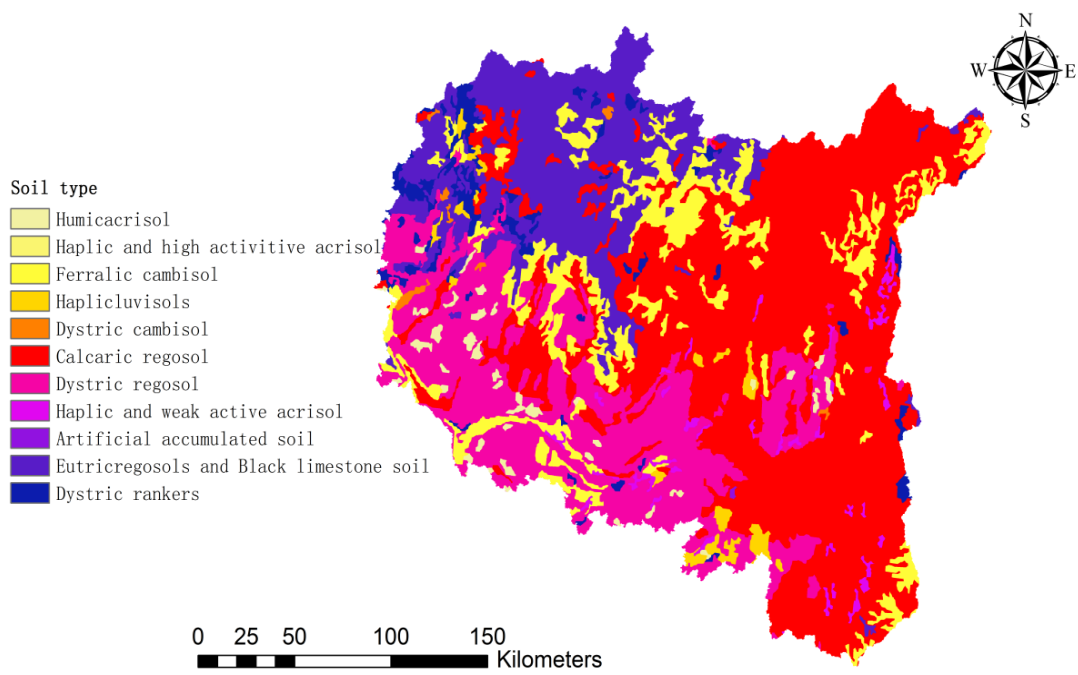
(a) DEM



522

523

(b) land use



524

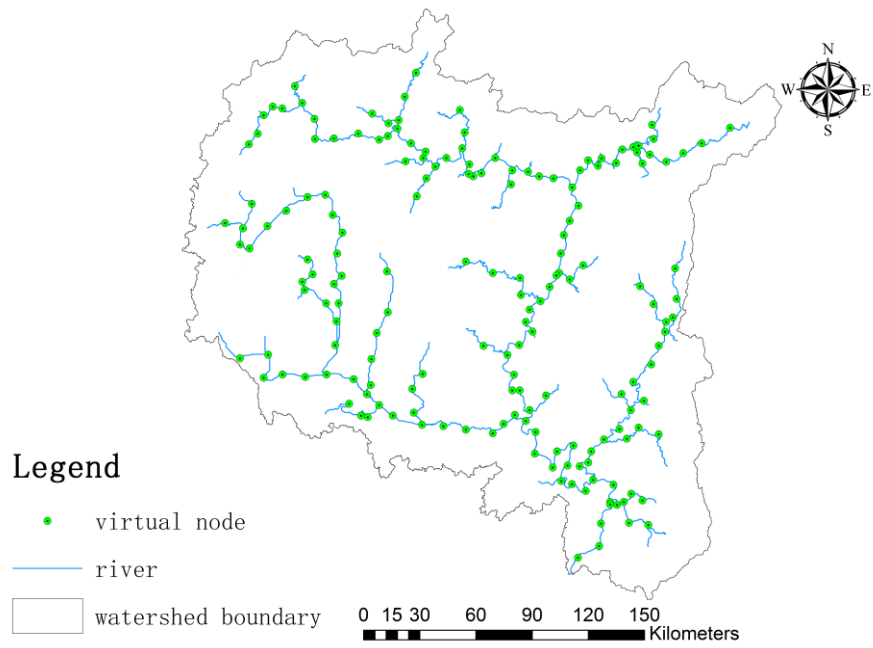
525

(c) soil type

526

Fig. 2 Terrain properties of LRB

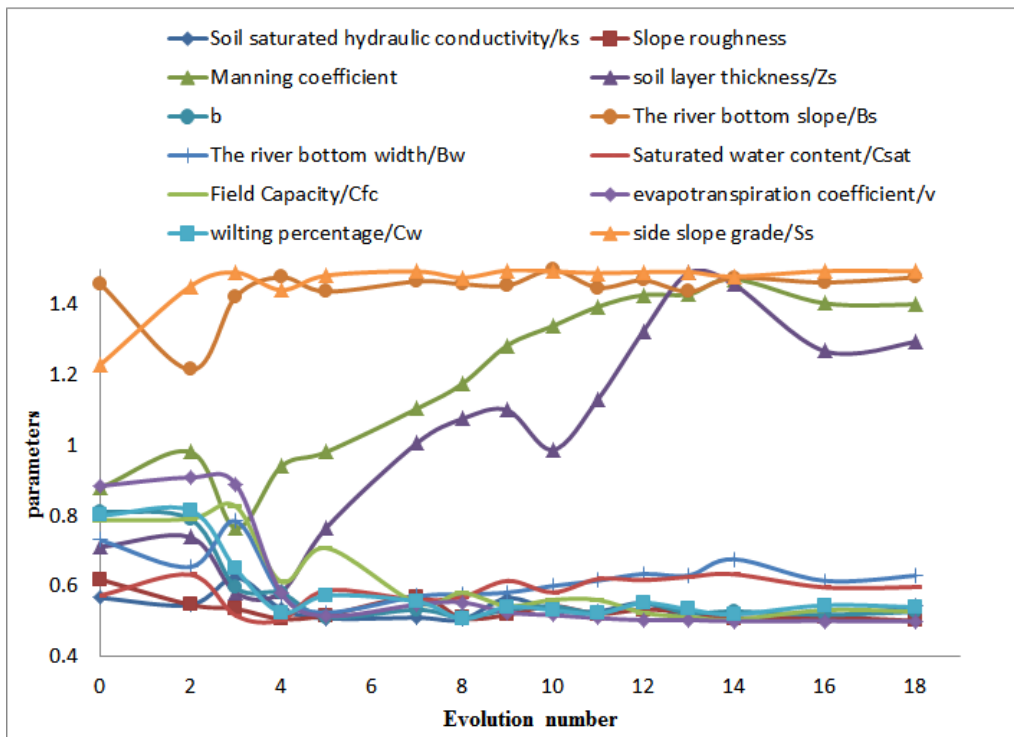
527



528

529 Fig. 3 Liuxihe Model structure set up for LRB (200m×200m resolution)

530



531

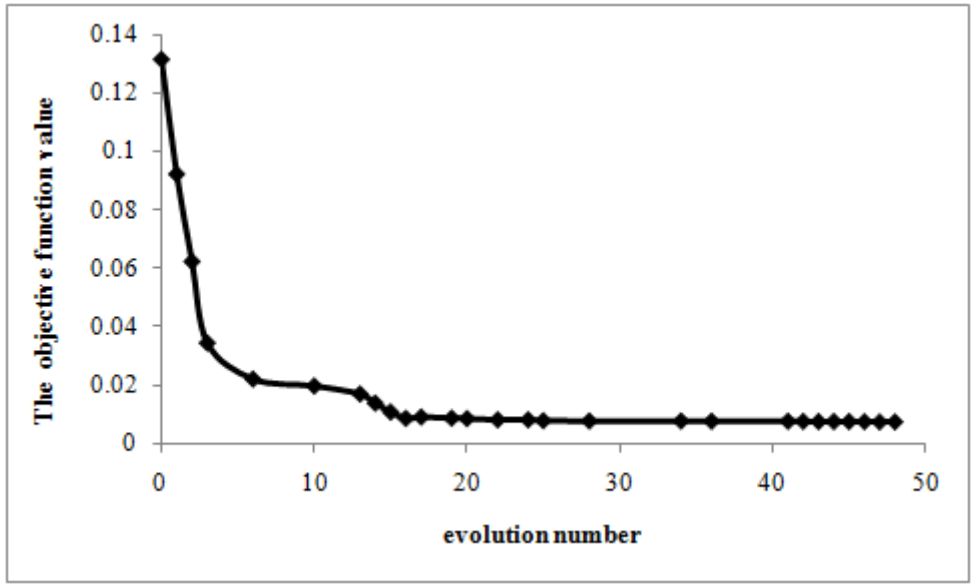
532

533

534

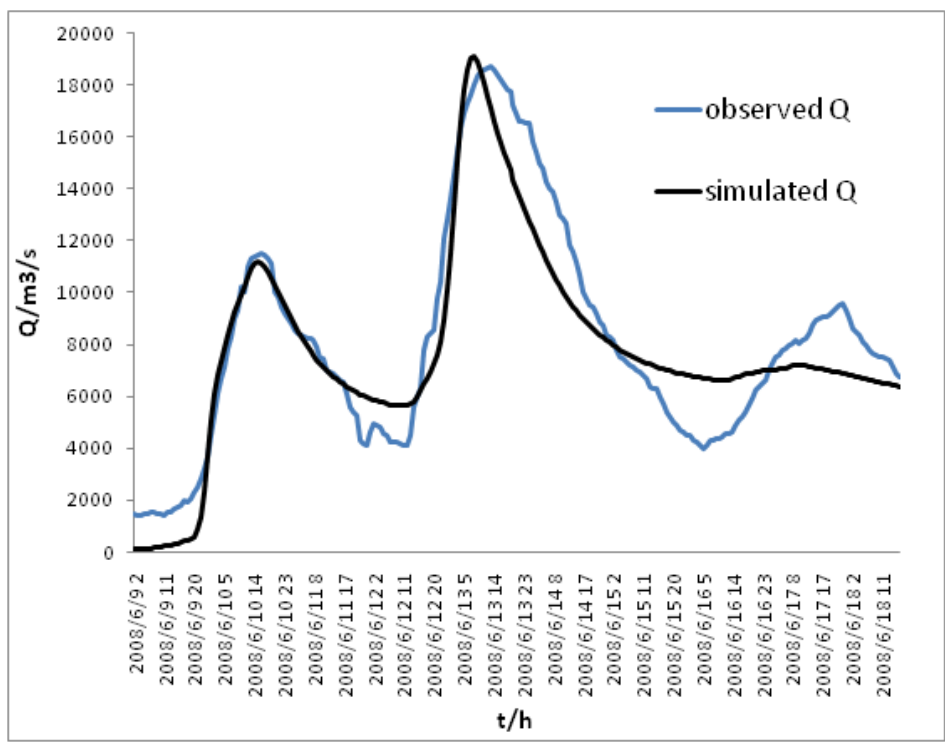
535

(a) Parameter evolution process



(b) Changing curve of objective function

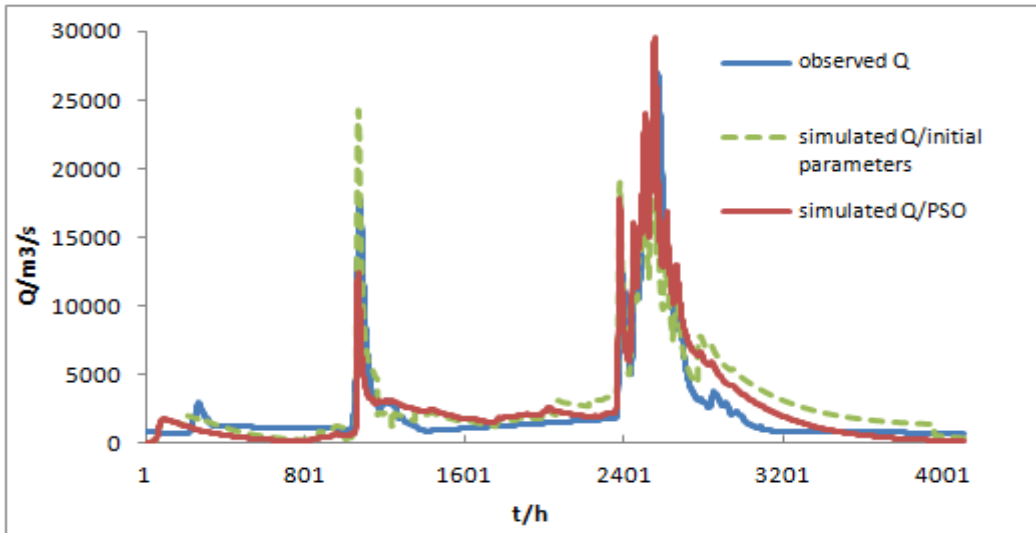
536
537
538
539



(c) Simulated flood process

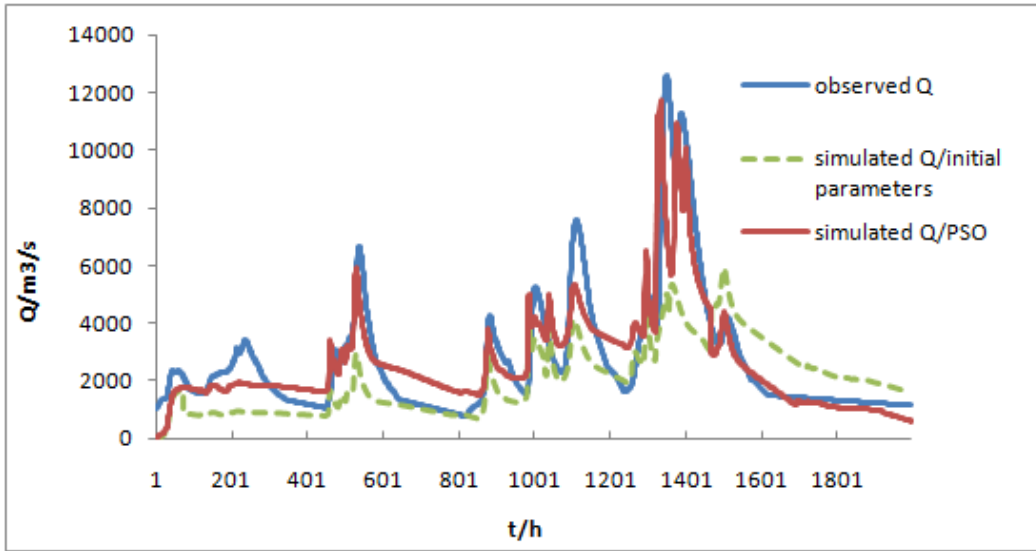
540
541
542
543

Fig. 4 Parameter optimization results of Liuxihe Model for LRB with PSO algorithm



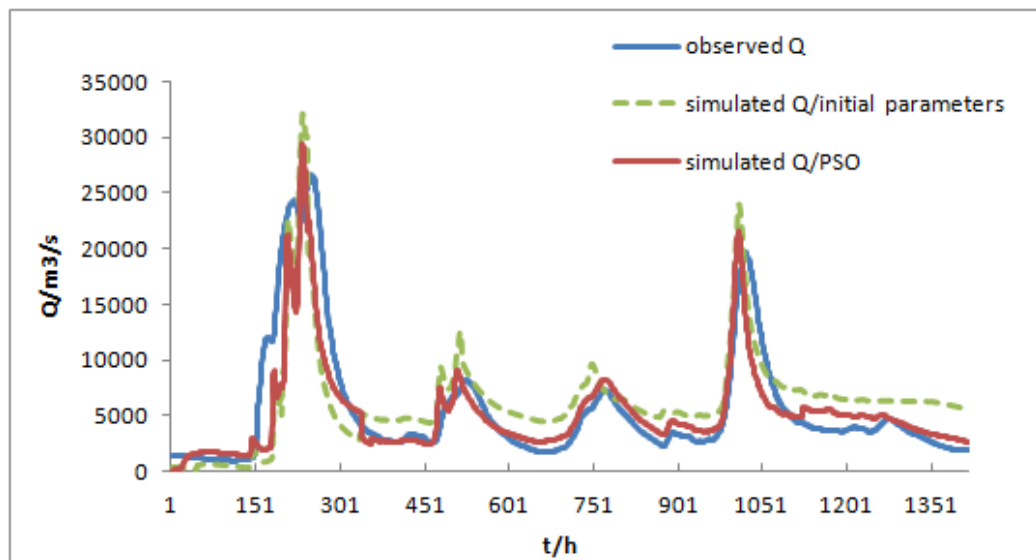
544
545

(a) flood event 1988051620



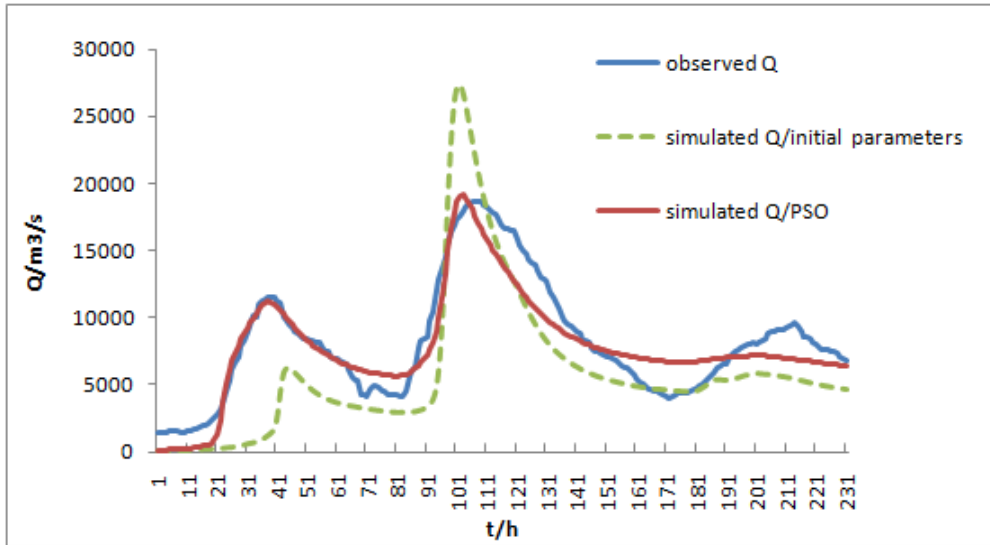
546
547

(b) flood event 1982042116



548
549

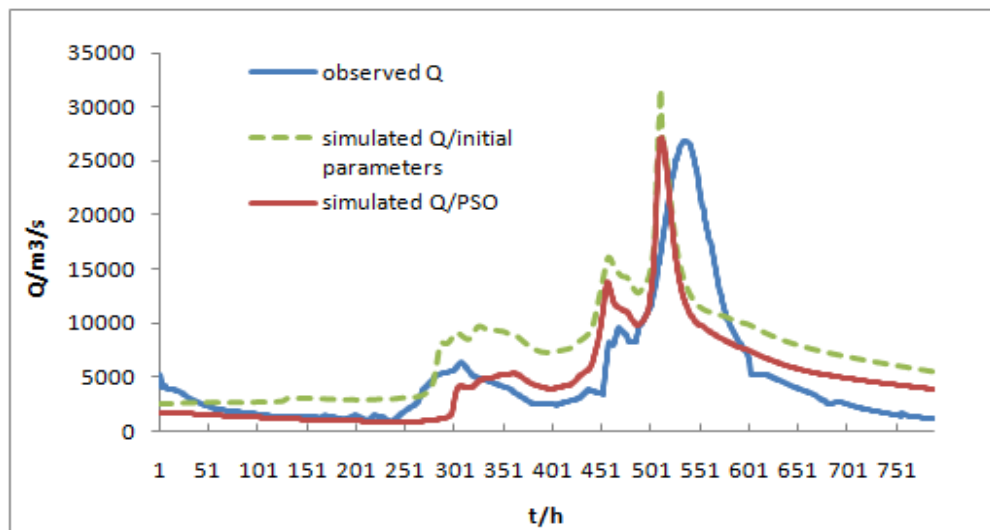
(c) flood event 1994060700



550

551

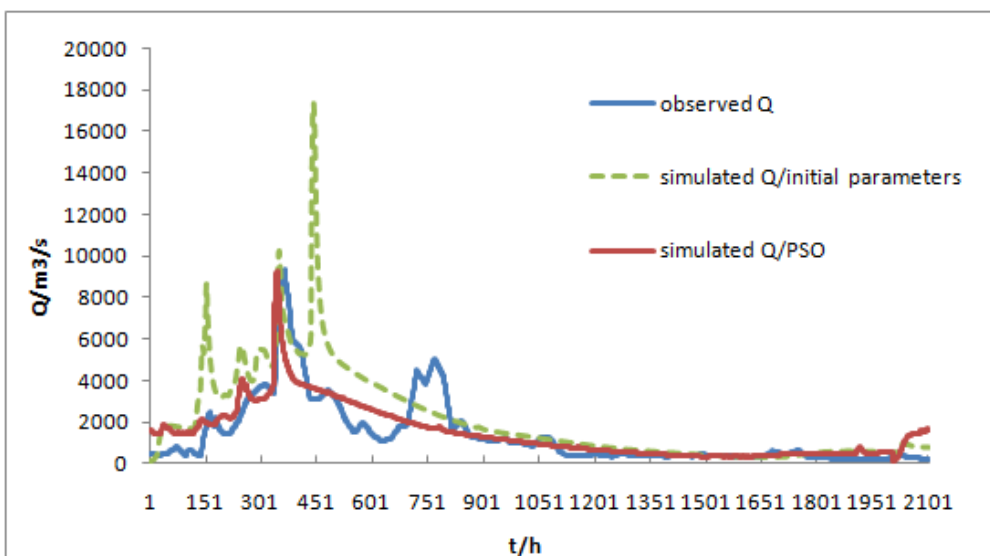
(d) flood event 2008060902



552

553

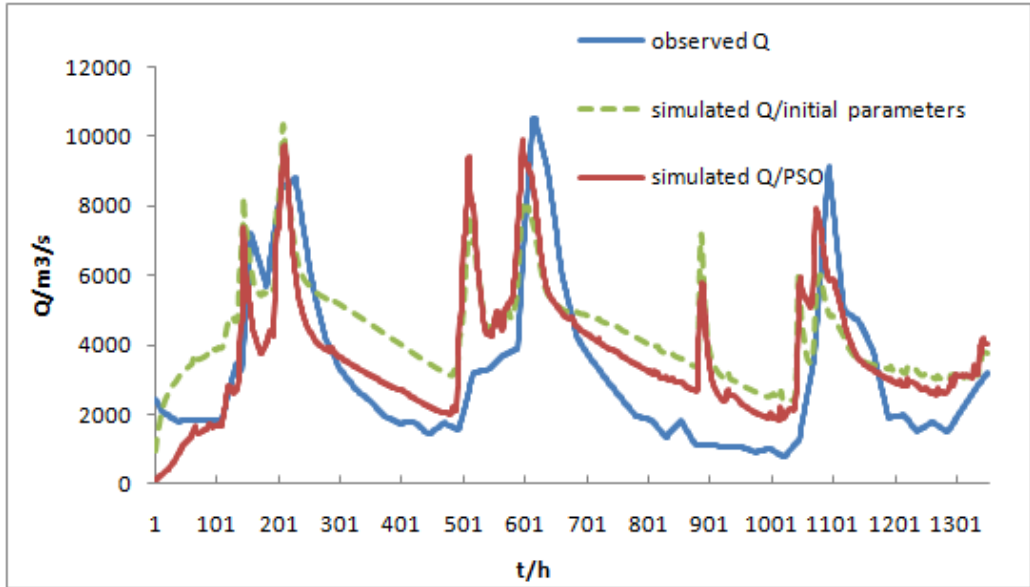
(e) flood event 200906090800



554

555

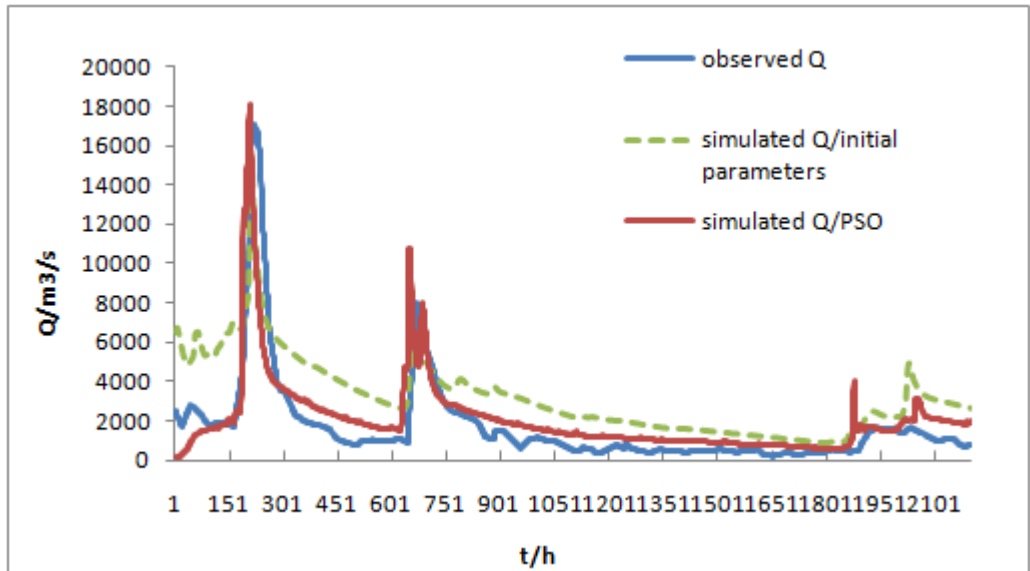
(f) flood event 201106010900



556

557

(g) flood event 201206022000



558

559

(h) flood event 201306011400

560

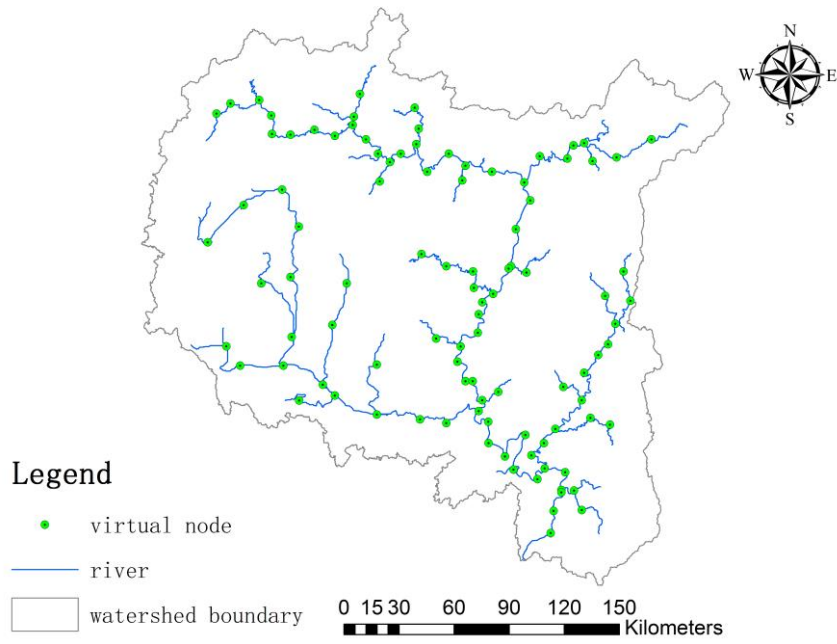
Fig. 5 Simulated flood events by Liuxihe Model with optimized parameters

561

562

563

564

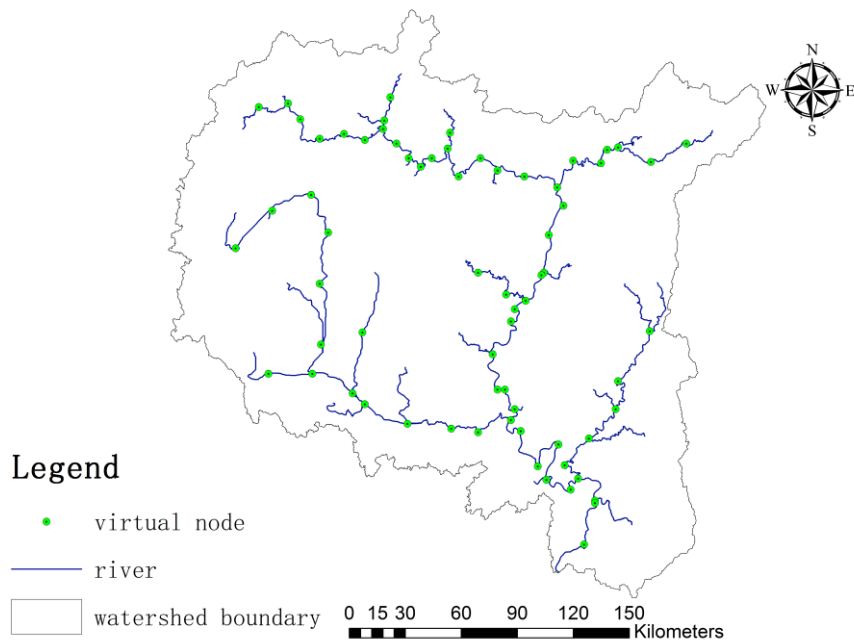


565

566

567

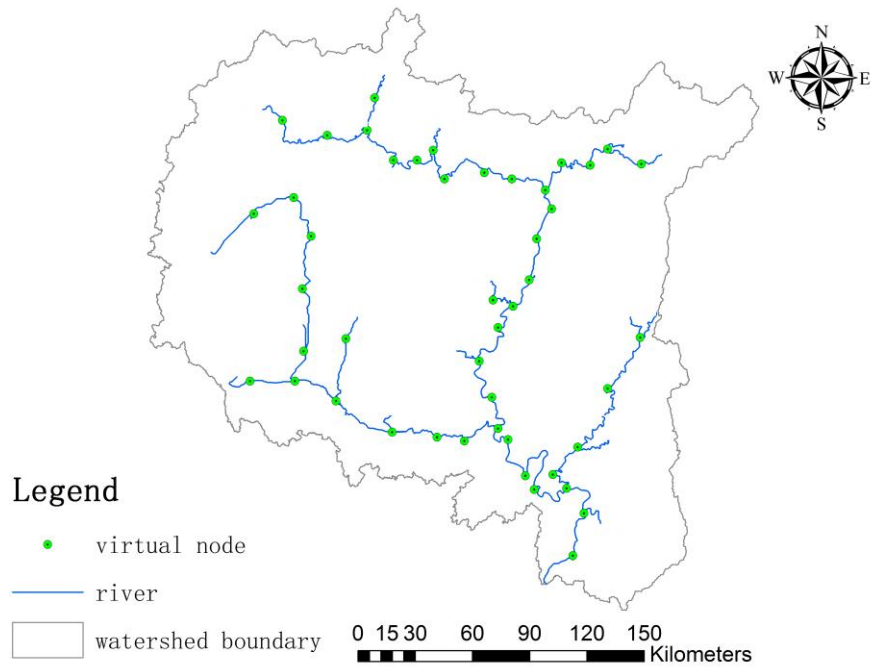
(a) 400m*400m resolution



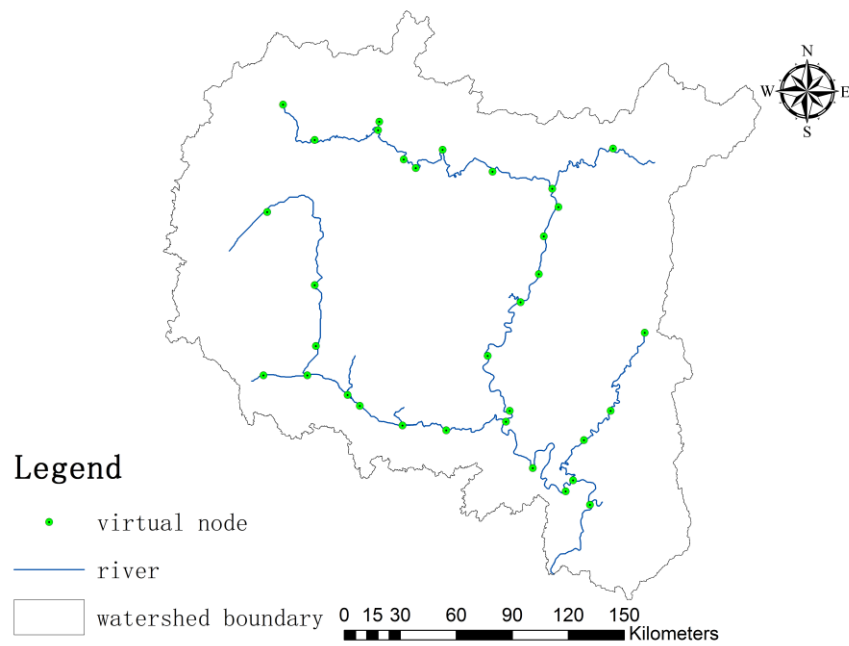
568

569

(b) 500m×500m resolution

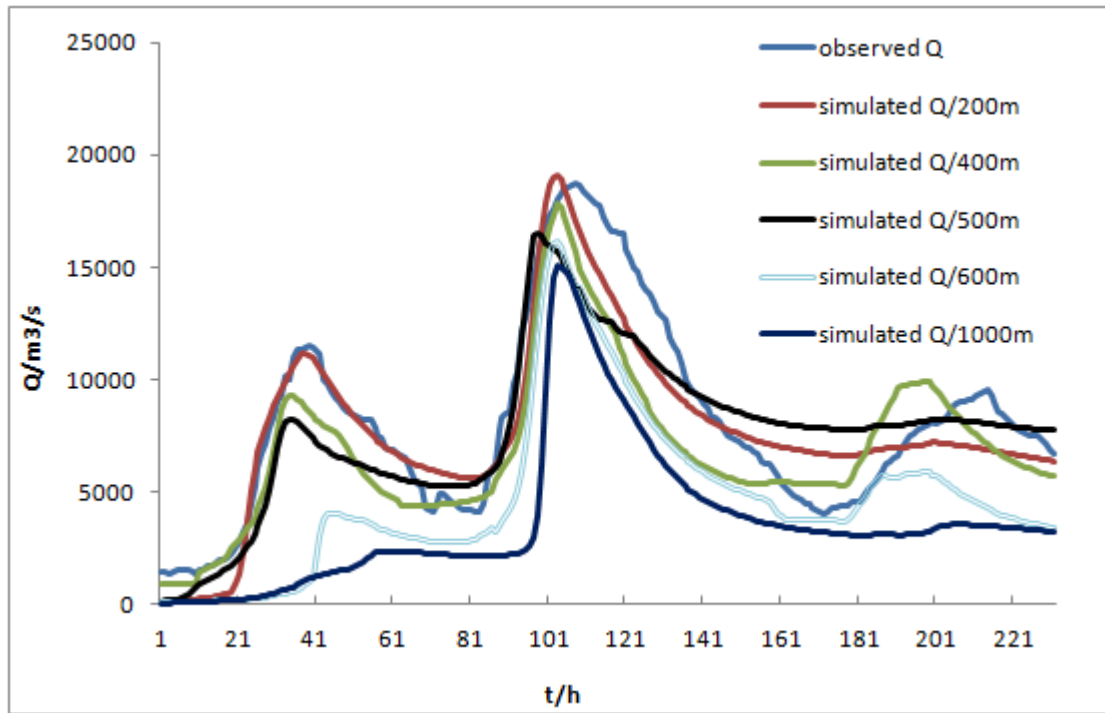


(c) 600m*600m resolution



(d) 1000m×1000m resolution

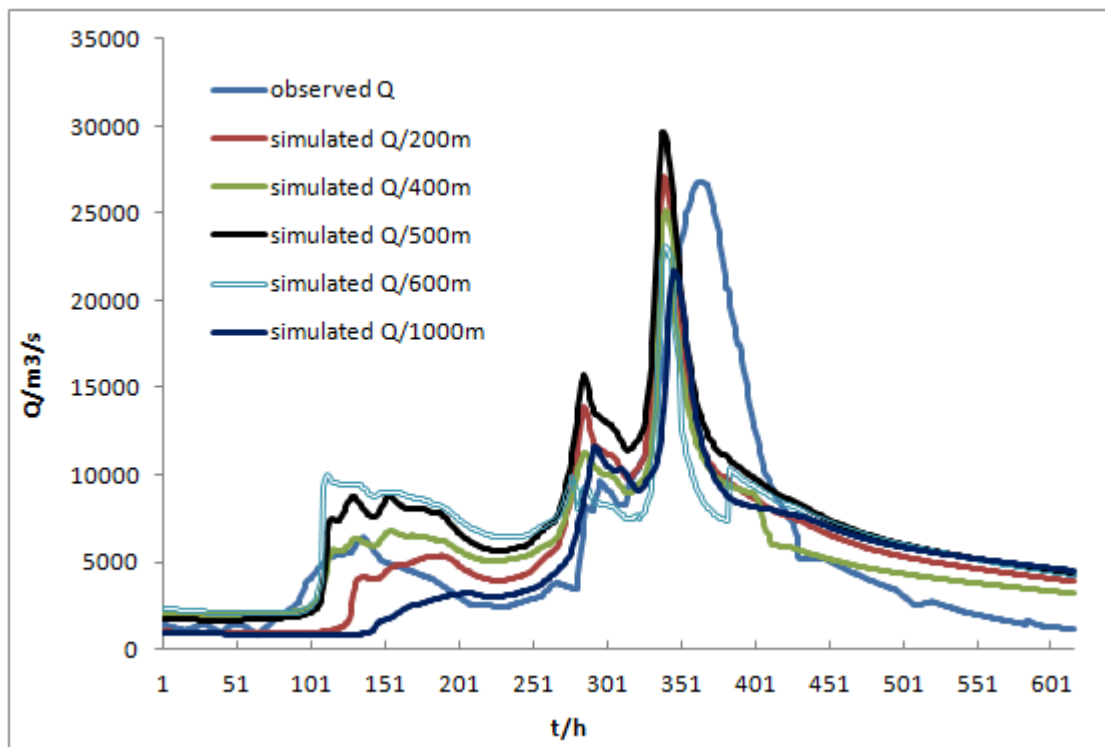
574 Fig. 6 Liuxihe Model structure set up for LRB with different resolution



575

576

(a) flood event 2008060902

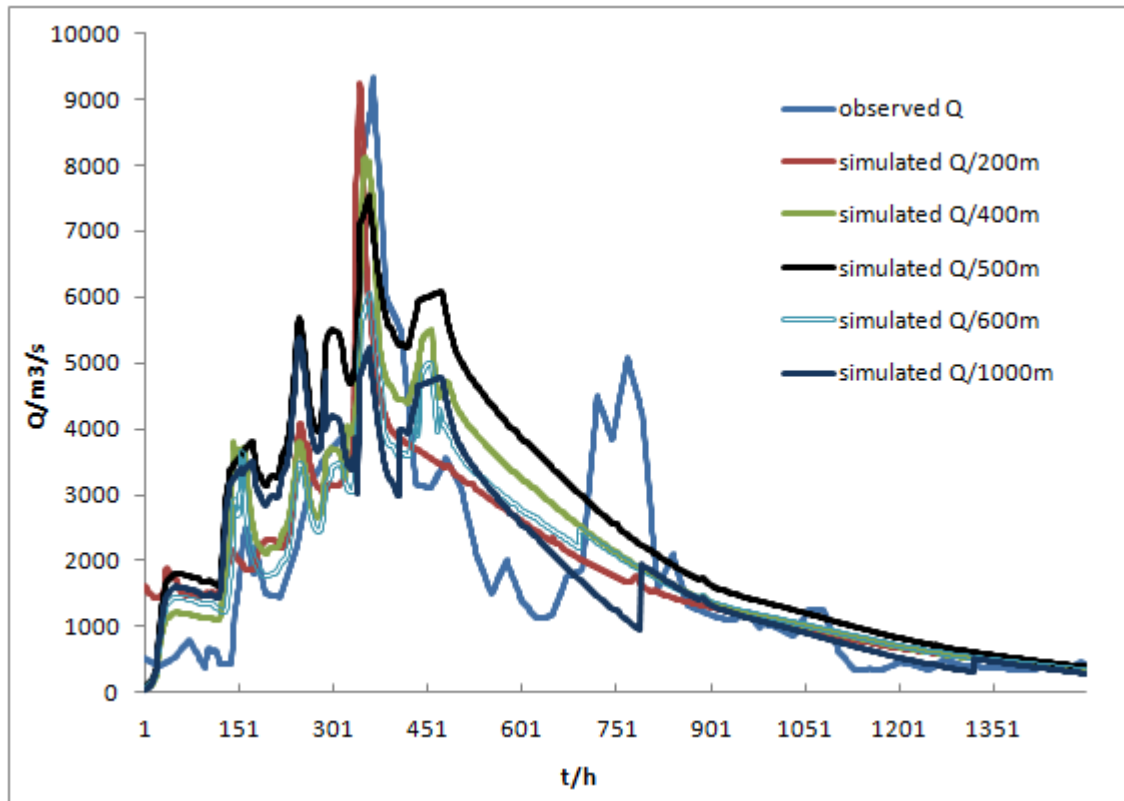


577

578

579

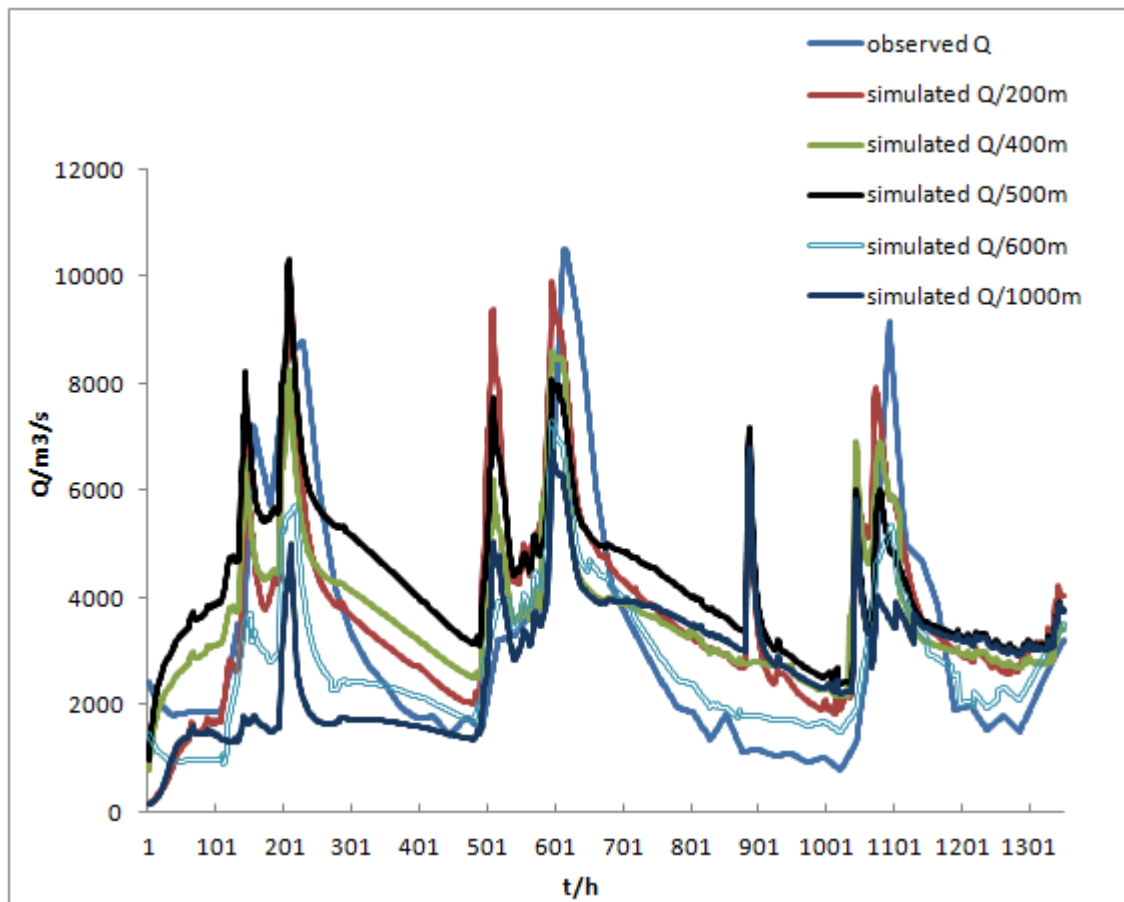
(b) flood event 2009060908



580

581

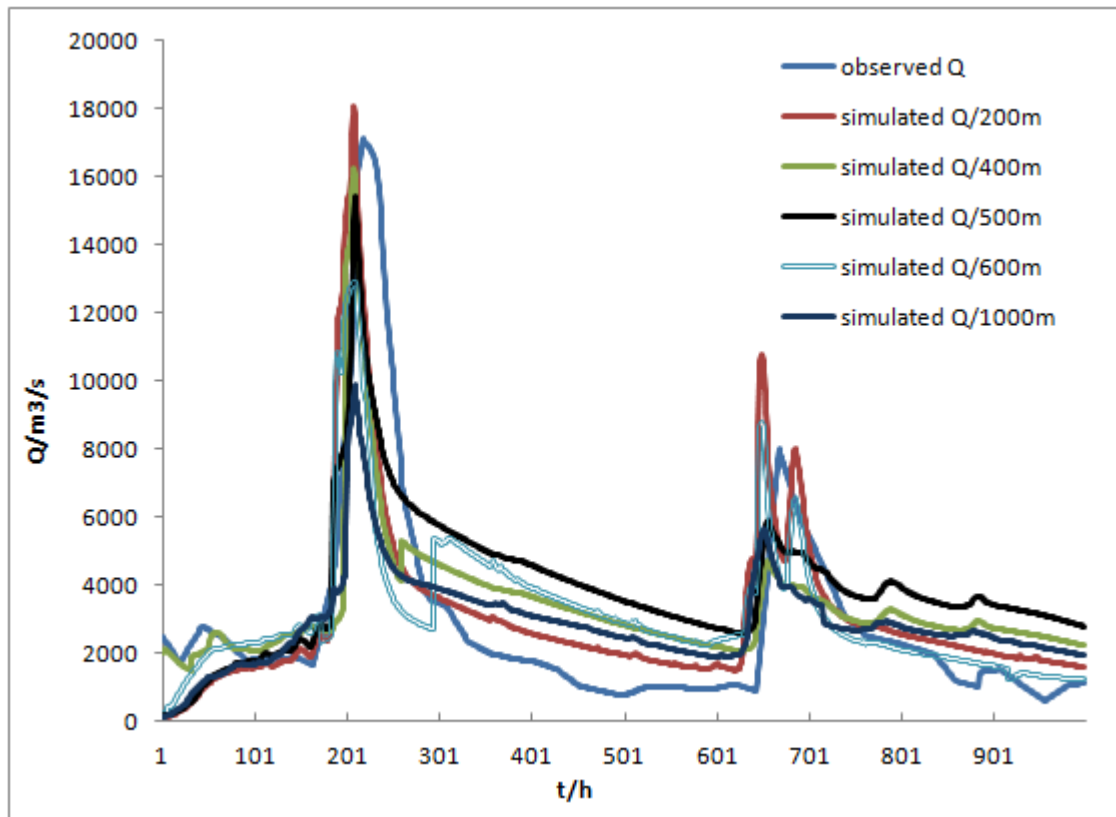
(c) flood event 2011060109



582

583

(d) flood event 2012060220



584

585

(e) flood event 2013060114

586

Fig. 7 Simulated results with different model resolutions

587

588

589 **Tables**

590

591

Table1 Brief information of flood events in LRB

<i>No.</i>	<i>Floods No.</i>	<i>Start time</i> (<i>yyyymmddhh</i>)	<i>End time</i> (<i>yyyymmddhh</i>)	<i>length of</i> <i>time/h</i>	<i>peak flow</i> (<i>m³/s</i>)
1	1982042116	1982042116	1982110216	4614	12600
2	1983020308	1983020308	1983021722	350	7880
3	1984021100	198402100	1984040105	1205	12900
4	1985011900	1985011900	1985021114	544	11400
5	1986022300	1986022300	1986042004	1334	12200
6	1987050100	1987050100	1987071700	1848	10800
7	1988070620	1988070620	1988100605	2915	27000
8	1989042600	1989042600	1989081009	2499	7500
9	1990050100	1990001000	1990072306	2006	11400
10	1991053118	1991053118	1991062806	686	14300
11	1992042900	1992042900	1992072107	1977	18100
12	1993060900	1993060900	1993082408	1818	21200
13	1994060700	1994060700	1994080706	1416	26500
14	1995052100	1995052100	1995071506	1296	17300
15	1996060600	1996060600	1996081808	1728	33700
16	1997060400	1997060400	1997062406	476	13600
17	1998051600	1998051600	1998090100	2520	19600
18	1990050100	1999050100	1999080404	1134	17800
19	2000052100	2000052100	2000061809	659	24100
20	2001051500	2001051500	2001062300	910	14200
21	2002042600	2002042600	2002081000	2520	17900
22	2003060600	2003060600	2003072103	843	11600
23	2004070300	200407000	2004081508	998	23700
24	2005061400	2005061400	2005070702	552	16400
25	2006060400	2006060400	2006071000	870	13200
26	2008060900	2008060900	2008061908	238	18700
27	2009060908	2009060908	2009071208	788	26800
28	2011061090	2011061009	2011090104	2004	9153
29	2012060220	2012060220	2012080101	1351	10500
30	2013060114	2013060114	2013090114	2200	17100

592

593

594

595

596
597
598

Table 2 The initial values of land use/cover related parameters

<i>Land use/cover</i>	<i>evaporation coefficient</i>	<i>roughness coefficient</i>
Evergreen needle leaf forest	0.7	0.4
Evergreen broadleaf forest	0.7	0.6
Shrubbery	0.7	0.4
Mountains and alpine meadow	0.7	0.2
Slope grassland	0.7	0.3
City	0.7	0.05
Cultivated land	0.7	0.35

599
600
601
602
603
604
605

Table 3 The initial values of soil related parameters

<i>Soil Type</i>	<i>soil thickness (mm)</i>	<i>water content at saturation condition</i>	<i>water content at field condition</i>	<i>hydraulic conductivity at saturation condition (mm/h)</i>
Humicacrisol	800	0.65	0.32	3.5
Haplic and high active acrisol	900	0.57	0.43	4.2
Ferralic cambisol	850	0.63	0.38	20.5
Haplicluvisols	980	0.46	0.15	2.6
Dystric cambisol	950	0.55	0.41	14
Calcaric regosol	1100	0.62	0.24	5.6
Dystric regosol	840	0.45	0.27	12.5
Haplic and weak active acrisol	1050	0.58	0.16	4.6
Artificial accumulated soil	1000	0.63	0.34	5.5
Eutricregosols and Black limestone	550	0.75	0.27	3.5
Dystric rankers	380	0.78	0.36	8

606
607
608
609
610

Table 4 Evaluation indices of the simulated flood events

ID	floods	parameters	Nash–Sutcliffe coefficient/C	Correlation coefficient/R	Process relative error/P	Peak flow relative error/E	Water balance coefficient/W
1	1982081219	initial	0.52	0.48	0.56	0.58	0.52
		optimized	0.84	0.75	0.30	0.01	0.83
2	1983020308	initial	0.60	0.55	0.45	0.26	0.65
		optimized	0.82	0.84	0.21	0.04	0.89
3	1984010100	initial	0.62	0.71	0.38	0.32	0.75
		optimized	0.75	0.89	0.26	0.14	0.96
4	1985010100	initial	0.58	0.57	0.35	0.33	0.85
		optimized	0.73	0.87	0.17	0.01	1.05
5	1986010100	initial	0.65	0.62	0.38	0.25	0.62
		optimized	0.83	0.85	0.23	0.04	0.94
6	1987050100	initial	0.76	0.45	0.35	0.36	0.58
		optimized	0.93	0.76	0.10	0.05	1.01
7	19880516200	initial	0.54	0.58	0.26	0.42	0.82
		optimized	0.84	0.80	0.15	0.04	0.90
8	1989042600	initial	0.52	0.55	0.55	0.25	0.62
		optimized	0.64	0.74	0.39	0.02	0.88
9	1990050100	initial	0.55	0.64	0.42	0.23	0.55
		optimized	0.85	0.87	0.14	0.03	0.85
10	1991053118	initial	0.63	0.62	0.40	0.18	0.68
		optimized	0.80	0.76	0.25	0.04	0.95
11	1992042900	initial	0.48	0.59	0.35	0.34	0.65
		optimized	0.66	0.84	0.20	0.11	0.89
12	1993060900	initial	0.75	0.65	0.38	0.28	0.84
		optimized	0.91	0.89	0.24	0.09	1.05
13	1994060700	initial	0.78	0.64	0.32	0.26	1.25
		optimized	0.93	0.85	0.14	0.04	0.85
14	1995052100	initial	0.68	0.48	0.42	0.35	0.65
		optimized	0.82	0.70	0.20	0.01	0.81
15	1996060600	initial	0.74	0.65	0.25	0.23	0.54
		optimized	0.90	0.93	0.18	0.02	0.86
16	1997060400	initial	0.65	0.51	0.23	0.26	0.65
		optimized	0.84	0.87	0.13	0.06	0.95
17	1998051600	initial	0.57	0.62	0.35	0.18	0.68
		optimized	0.83	0.85	0.30	0.01	1.05
18	1999061700	initial	0.48	0.59	0.33	0.15	0.55
		optimized	0.60	0.83	0.15	0.05	0.80
19	2000052100	initial	0.67	0.62	0.45	0.25	0.58
		optimized	0.79	0.89	0.26	0.06	0.83

20	2001051500	initial	0.62	0.56	0.32	0.22	0.68
		optimized	0.80	0.82	0.25	0.07	0.82
21	2002042600	initial	0.68	0.65	0.38	0.18	0.57
		optimized	0.86	0.90	0.24	0.02	0.87
22	2003060600	initial	0.75	0.55	0.25	0.26	0.55
		optimized	0.92	0.85	0.14	0.04	0.76
23	2004070300	initial	0.58	0.68	0.38	0.27	0.68
		optimized	0.78	0.82	0.23	0.08	0.85
24	2005061400	initial	0.65	0.62	0.52	0.32	0.65
		optimized	0.76	0.76	0.35	0.06	0.74
25	2006060400	initial	0.68	0.72	0.62	0.35	0.53
		optimized	0.82	0.83	0.30	0.10	0.86
26	2009060908	initial	0.75	0.78	0.25	0.23	1.22
		optimized	0.95	0.92	0.17	0.04	0.09
27	2011010100	initial	0.66	0.75	0.35	0.55	1.66
		optimized	0.80	0.84	0.26	0.03	1.02
28	2012010100	initial	0.63	0.68	0.34	0.22	1.42
		optimized	0.82	0.79	0.20	0.05	0.80
29	2013010100	initial	0.78	0.65	0.31	0.32	1.35
		optimized	0.95	0.82	0.20	0.06	0.92
average		initial	0.64	0.62	0.37	0.29	0.78
		optimized	0.82	0.83	0.22	0.05	0.87

613

614

615

616 Table 5 Grid cell numbers with different model spatial resolution

Model resolution	Number of grid cells	Number of hill slope cells	Number of river cells
200m*200m	1469900	1463204	6696
400m*400m	367475	365801	1674
500m*500m	235184	234113	1071
600m*600m	163322	162578	744
1000m*1000m	58796	58528	268

617

618

619

622 Table 6 Optimized parameters with different model spatial resolution*

Resolution	Soil saturated hydraulic conductivity/ks	Slope roughness	Manning coefficient	Soil layer thickness/Zs	b	The river bottom slope/Bs
	1.33	0.66	1.19	1.42	0.67	0.75
200m	The river bottom width/Bw	Saturated water content/Csat	Field Capacity/Cfc	Evapotranspiration coefficient/v	Wilting percentage/Cw	Side slope grade/Ss
	1.24	1.11	1.2	0.94	0.68	1.42
400m	Soil saturated hydraulic conductivity/ks	Slope roughness	Manning coefficient	Soil layer thickness/Zs	b	The river bottom slope/Bs
	0.75	1.12	1.23	1.4	1.25	0.65
400m	The river bottom width/Bw	Saturated water content/Csat	Field Capacity/Cfc	Evapotranspiration coefficient/v	Wilting percentage/Cw	Side slope grade/Ss
	0.89	1.02	1.22	1.18	1.15	0.76
500m	Soil saturated hydraulic conductivity/ks	Slope roughness	Manning coefficient	Soil layer thickness/Zs	b	The river bottom slope/Bs
	0.67	1.47	1.49	1.37	1.5	0.51
500m	The river bottom width/Bw	Saturated water content/Csat	Field Capacity/Cfc	Evapotranspiration coefficient/v	Wilting percentage/Cw	Side slope grade/Ss
	0.91	1.16	1.41	1.37	1.37	0.5
600m	Soil saturated hydraulic conductivity/ks	Slope roughness	Manning coefficient	Soil layer thickness/Zs	b	The river bottom slope/Bs
	1.02	0.98	1.24	0.95	1.21	0.86

	The river bottom width/Bw	Saturated water content/Csat	Field Capacity/Cfc	Evapotranspiration coefficient/v	Wilting percentage/Cw	Side slope grade/Ss
	1.12	0.87	1.28	1.08	1.16	0.95
	Soil saturated hydraulic conductivity/ks	Slope roughness	Manning coefficient	Soil layer thickness/Zs	b	The river bottom slope/Bs
1000m	0.5	1.43	1.17	1.11	1.47	0.57
	The river bottom width/Bw	Saturated water content/Csat	Field Capacity/Cfc	Evapotranspiration coefficient/v	Wilting percentage/Cw	Side slope grade/Ss
	1.1	0.76	0.53	0.6	1.5	0.54

623 *Values in the table are adjusting coefficient of the optimized parameters to the initial
624 parameters, so values of the final optimized parameters are initial parameters time adjusting
625 coefficient.

626

- 628 [1] Abbott, M.B. et al.: An Introduction to the European Hydrologic System-System Hydrologue European,
629 'SHE', a: History and Philosophy of a Physically-based, Distributed Modelling System, Journal of
630 Hydrology, 87, 45-59, 1986.
- 631 [2] Abbott, M.B. et al.: An Introduction to the European Hydrologic System-System Hydrologue European,
632 'SHE', b: Structure of a Physically based, distributed modeling System, Journal of Hydrology, 87, 61-77,
633 1986.
- 634 [3] Ambrose, B., Beven, K., and Freer, J.: Toward a generalization of the TOPMODEL concepts: Topographic
635 indices of hydrologic similarity, Water Resour. Res., 32, 2135-2145, 1996.
- 636 [4] Anderson, A. N., McBratney, A. B., and FitzPatrick, K. E. A soil mass, surface and spectral fractal dimensions
637 estimated from thin section photographs. Soil Sci. Soc. Am. J., 60, 962-969, 1996.
- 638 [5] Arya, L.M., and J.F. Paris. 1981. A physioempirical model to predict the soil moisture characteristic from
639 particle-size distribution and bulk density data. Soil Sci. Soc. Am. J. 45, 1023-1030.
- 640 [6] Bartholmes, J.C., Thielen, J., Ramos, M.H., Gentilini, S., 2009. The european flood alert system EFAS e part
641 2: statistical skill assessment of probabilistic and deterministic operational forecasts. Hydrol. Earth Syst. Sci.
642 13 (2), 141e153.
- 643 [7] Burnash, R. J. C., 1995. "The NWS river forecast system-catchment modeling." Computer models of
644 watershed hydrology, V. P. Singh, ed., Water Resource Publications, Littleton, Colo., 311-366.
- 645 [8] Catto  n, C  dine, Hilary McMillan, and Stuart Moore. Coupling a high-resolution weather model with a
646 hydrological model for flood forecasting in New Zealand[J]. Journal of Hydrology (NZ), 2016,55 (1): 1-23.
- 647 [9] Chen, Xiuwan, Analysis on flood disasters in China, 1995. Marine Geology and Quaternary Geology,
648 15(3):161-168.
- 649 [10] Chen, Huiquan, Mao Shimin. Calculation and Verification of an Universal Water Surface Evaporation
650 Coefficient Formula[J]. Advances in Water Science, 1995, 6(2):116-120.
- 651 [11] Chen, Yangbo. Liuxihe Model, China Science and Technology Press, September 2009.
- 652 [12] Chen, Yangbo, Ren, Q.W., Huang, F.H., Xu, H.J., and Cluckie, I.: Liuxihe Model and its modeling to river
653 basin flood, Journal of Hydrologic Engineering, 16, 33-50, 2011.
- 654 [13] Chen, Yangbo, Yi Dong, Pengcheng Zhang. Study on the method of flood forecasting of small and medium
655 sized catchment, proceeding of the 2013 annual meeting of the Chinese Society of Hydraulic Engineering,
656 1001-1008, 2013.
- 657 [14] Chen, Yangbo, Ji Li, Huijun Xu. Improving flood forecasting capability of physically based distributed
658 hydrological model by parameter optimization. Hydrology & Earth System Sciences, 20, 375-392, 2016.
- 659 [15] Dibike, Y. B., P. Coulibaly. Hydrologic impact of climate change in the Saguenay watershed: comparison of
660 downscaling methods and hydrologic models[J]. Journal of Hydrology, 2005, 307(1-4): 145-163.
- 661 [16] EEA, 2010. Mapping the Impacts of Natural Hazards and Technological Accidents in Europe: an Overview
662 of the Last Decade. EEA Technical Report. European Environment Agency, Copenhagen, p. 144.
- 663 [17] Falorni, G., Teles, V., Vivoni, E. R., Bras, R. L., and Amaratunga, K. S.: Analysis and characterization of the
664 vertical accuracy of digital elevation models from the Shuttle Radar Topography Mission, J. Geophys. Res.
665 F-Earth Surf., 110, F02005, doi:10.1029/2003JF000113, 2005.
- 666 [18] Freeze, R. A., and Harlan, R.L.: Blueprint for a physically-based, digitally simulated, hydrologic response
667 model, Journal of Hydrology, 9, 237-258, 1969.
- 668 [19] Grayson, R.B., Moore, I. D., and McMahon, T.A.: Physically based hydrologic modeling: I. A Terrain-based
669 model for investigative purposes, Water Resources Research, 28, 2639-2658, 1992.
- 670 [20] Guo, Hanqing, Hua Youzhi, Bai Xiumei. Hydrological Effects of Litter on Different Forest Stands and Study
671 about Surface Roughness Coefficient[J]. Journal of Soil and Water Conservation, 2010, 24(2): 179-183
- 672 [21] Jensen, S. K. and J. O. Domingue, 1988, Extracting Topographic Structure from Digital Elevation Data for
673 Geographic Information System Analysis, Photogrammetric Engineering and Remote Sensing, 54(11)
- 674 [22] Jia, Y., Ni, G., and Kawahara, Y.: Development of WEP model and its application to an urban watershed,
675 Hydrological Processes, 15, 2175- 2194, 2001.
- 676 [23] Julien, P.Y., Saghafian, B., and Ogden, F. L.: Raster-Based Hydrologic Modeling of spatially-Variied Surface
677 Runoff, Water Resources Bulletin, 31, 523-536, 1995.
- 678 [24] Kauffeldt, A., F. Wetterhall, F. Pappenberger, P. Salamon, J. Thielen. Technical review of large-scale
679 hydrological models for implementation in operational flood forecasting schemes on continental level[J].
680 Environmental Modelling & Software, 2016, 75: 68-76.
- 681 [25] Kavvas, M., Chen, Z., Dogrul, C., Yoon, J., Ohara, N., Liang, L., Aksoy, H., Anderson, M., Yoshitani, J.,
682 Fukami, K., and Matsuura, T. (2004). "Watershed Environmental Hydrology (WEHY) Model Based on
683 Upscaled Conservation Equations: Hydrologic Module." J. Hydrol. Eng.,
684 10.1061/(ASCE)1084-0699(2004)9:6(450), 450-464.
- 685 [26] Kouwen, N.: WATFLOOD: A Micro-Computer based Flood Forecasting System based on Real-Time
686 Weather Radar, Canadian Water Resources Journal, 13, 62-77, 1988.
- 687 [27] Krzmm, R. W. The Federal Role in Natural Disasters. International Symposium on Torrential Rain and
688 Flood, Oct 5-9, 1992, Huangshan, China.
- 689 [28] Kuniyoshi, T. Japanese Experiences of Combating Against Floods in the past half century. International
690 Symposium on Torrential Rain and Flood, Oct 5-9, 1992, Huangshan, China.

- 691 [29] Li, Y., C. Wang. Impacts of urbanization on surface runoff of the Dardenne Creek watershed, St. Charles
692 County, Missouri[J]. *Phys. Geogr.* 2009, 30(6):556-573.
- 693 [30] Li, Yuting, Zhang Jianjun, Ri Hao, et al. Effect of Different Land Use Types on Soil Anti-scourability and
694 Roughness in Loess Area of Western Shanxi Province[J]. *Journal of Soil and Water Conservation*, 2013,
695 27(4):1-6.
- 696 [31] Liang, X., Lettenmaier, D.P., Wood, E.F., and Burges, S.J.:A simple hydrologically based model of land
697 surface water and energy fluxes for general circulation models, *J. Geophys. Res.*, 99,14415-14428,1994.
- 698 [32] Liao, Zhenghong, Yangbo Chen, Xu Huijun, Yan Wanling, Ren Qiwei, Parameter Sensitivity Analysis of the
699 Liuxihe Model Based on E-FAST Algorithm, *Tropical Geography*, 2012, 32(6):606-612.
- 700 [33] Liao, Zhenghong, Yangbo Chen, Xu Huijun, He Jinxiang, Study of Liuxihe Model for flood forecast of
701 Tiantoushui Watershed, Yangtze River, 2012, 43(20): 12-16.
- 702 [34] Lohmann, D., Raschke, E., Nijssen, B., Lettenmaier, D. P. (1998). Regional scale hydrology: II. Application
703 of the VIC-2L model to the Weser River, Germany, *Hydrological Sciences Journal*, 43:1, 143-158.
- 704 [35] Loveland, T. R., Merchant, J. W., Ohlen, D. O., and Brown, J. F.:Development of a Land Cover
705 Characteristics Data Base for the Conterminous U.S., *Photogram. Eng. Remote Sens.*, 57, 1453–1463, 1991.
- 706 [36] Loveland, T. R., Reed, B. C., Brown, J. F., Ohlen, D. O., Zhu, J., Yang, L., and Merchant, J. W.:
707 Development of a Global Land Cover Characteristics Database and IGBP DISCover from 1-km AVHRR
708 Data, *Int. J. Remote Sens.*, 21, 1303–1330, 2000.
- 709 [37] Madsen, H.:Parameter estimation in distributed hydrological catchment modelling using automatic
710 calibration with multiple objectives, *Advances in Water Resources*, 26,205-216, 2003.
- 711 [38] Olivera, F., B. B. DeFee. Urbanization and its effect on runoff in the Whiteoak Bayou Watershed, Texas[J]. *J.*
712 *Am. Water Resour. Assoc.* , 2007, 43(1):170-182.
- 713 [39] Ott, B., Uhlenbrook S. Quantifying the impact of land-use changes at the event and seasonal time scale using
714 a process-oriented catchment model[J]. *Hydrol Earth Syst Sci.* ,2004, 8:62-78.
- 715 [40] Refsgaard, J. C.,1997. “Parameterisation, calibration and validation of distributed hydrological models.” *J.*
716 *Hydrol.*, 198, 69–97.
- 717 [41] Rose, Seth Norman E. Peters. Effects of urbanization on streamflow in the Atlanta area (Georgia, USA): a
718 comparative hydrological Approach[J]. *Hydrological Processes*, 2001, 15(8):1141-1157.
- 719 [42] Rwetabula, J., F. De Smedt, M. Rebhun. Prediction of runoff and discharge in the Simiyu River (tributary of
720 Lake Victoria, Tanzania) using the WetSpa model. *Hydrology and Earth System Sciences Discussions*,
721 *European Geosciences Union*, 2007, 4 (2):881-908.
- 722 [43] Shafii, M. and Smedt, F. De: Multi-objective calibration of a distributed hydrological model (WetSpa) using
723 a genetic algorithm, *Hydrol. Earth Syst. Sci.*, 13, 2137–2149, 2009.
- 724 [44] Sharma, A. Tiwari, K. N.: A comparative appraisal of hydrological behavior of SRTM DEM at catchment
725 level, *J. Hydrol.*, 519, 1394–1404, 2014.
- 726 [45] Shen, Shengqiong, Shuanghe, Guze. Conversion Coefficient between Small Evaporation Pan and
727 Theoretically Calculated Water Surface Evaporation in China[J].*Journal of Nanjing Institute of Meteorology*,
728 2007, 30(4):561-565.
- 729 [46] Sood, A., Smakhtin, V., 2015. Global hydrological models: a review. *Hydrol. Sci. J.* 60(4), 549e565.
730 <http://dx.doi.org/10.1080/02626667.2014.950580>.
- 731 [47] Stisen, Simon, Jensen, Karsten H., Inge Sandholt , David I.F. Grimes. A remote sensing driven distributed
732 hydrological model of the Senegal River basin, *Journal of Hydrology*, 2008(354):131-148.
- 733 [48] Strahler, A. N.Quantitative analysis of watershed Geomorphology, *Transactions of the American Geophysical*
734 *Union*, 1957, 35(6), 913-920.
- 735 [49] Sugawara, M. _1995_. “Tank model.” *Computer models of watershed hydrology*, V. P. Singh, ed., *Water*
736 *Resources Publications*, Littleton, Colo., 165–214.
- 737 [50] Thielen, J., Bartholmes, J., Ramos, M.H., de Roo, A., 2009. The European flood alert system e part 1:
738 concept and development. *Hydrol. Earth Syst. Sci.* 13 (2), 125-140.
- 739 [51] Thielen, J., Pappenberger, F., Salamon, P., Bogner, K., Burek, P., de Roo, A., 2010. The State of the Art of
740 Flood Forecasting–Hydrological Ensemble Prediction Systems, p. 145.
- 741 [52] Todini, E., 1996. “The ARNO rainfall-runoff model.” *J. Hydrol.*, 175, 339–382.
- 742 [53] Vanrheenen, N. T., A W Wood, R N Palmer, et al. Potential implications of PCM climate change scenarios for
743 Sacramento-San Joaquin River Basin hydrology and water resources[J]. *Climatic Change*, 2004, 62(1-3):
744 257-281.
- 745 [54] Vieux, B. E., and Vieux, J. E.:VfloTM: A Real-time Distributed Hydrologic Model[A]. In:Proceedings of the
746 2nd Federal Interagency Hydrologic Modeling Conference, July 28-August 1, Las Vegas, Nevada. Abstract
747 and paper on CD-ROM, 2002.
- 748 [55] Vieux, B.E., Moreda, F.G.:Ordered physics-based parameter adjustment of a distributed model. In: Duan, Q.,
749 Sorooshian, S., Gupta, H.V., Rousseau, A.N., Turcotte, R. (Eds.), *Advances in Calibration of Watershed*
750 *Models. Water Science and Application Series*, vol. 6. American Geophysical Union, pp. 267-281, 2003
- 751 [56] Vieux, B.E., Cui Z., Gaur A.: Evaluation of a physics-based distributed hydrologic model for flood
752 forecasting, *Journal of Hydrology*, 298, 155-177, 2004.
- 753 [57] Vivoni, E.R., Ivanov, V.Y., Bras, R.L. and Entekhabi, D. 2004. Generation of Triangulated Irregular
754 Networks based on Hydrological Similarity. *Journal of Hydrologic Engineering*. 9(4): 288-302.
- 755 [58] Wang, Z., Batelaan, O., De Smedt, F.: A distributed model for water and energy transfer between soil, plants
756 and atmosphere (WetSpa). *Journal of Physics and Chemistry of the Earth* 21, 189-193, 1997.

- 757 [59] Wigmosta, M. S., Vai, L. W., and Lettenmaier, D. P.: A Distributed Hydrology-Vegetation Model for
758 Complex Terrain, *Water Resources Research*, 30,1665-1669,1994.
- 759 [60] Witold F. Krajewski, Daniel Ceynar, Ibrahim Demir, Radoslaw Goska, Anton Kruger, Carmen Langel,
760 Ricardo Mantilla, James Niemeier, Felipe Quintero, Bong-Chul Seo, Scott J. Small, Larry J. Weber, and
761 Nathan C. Young. Real-time Flood Forecasting and Information System for the State of Iowa[J] *Bull.*
762 *Amer.Meteor. Soc.* doi:10.1175/BAMS-D-15-00243.1, in press.
- 763 [61] Xu, Huijuna, Yangbo Chen, Zeng Biqiu, He Jinxiang, Liao Zhenghong, Application of SCE-UA Algorithm
764 to Parameter Optimization of Liuxihe Model, *Tropical Geography*, 2012.1, 32(1): 32-37.
- 765 [62] Xu, Huijun, Yangbo Chen, Li Zhouyang, He Jinxiang, Analysis on parameter sensitivity of distributed
766 hydrological model based on LH-OAT Method, *Yangtze River*, 2012, 43(7): 19-23.
- 767 [63] Yang, D., Herath ,S. and Musiaka, K.:Development of a geomorphologic properties extracted from DEMs
768 for hydrologic modeling, *Annual journal of Hydraulic Engineering*, JSCE, 47,49-65,1997.
- 769 [64] Zaradny, H. *Groundwater Flow in Saturated and Unsaturated Soil*. Now York:A A BalKema,1993.
- 770 [65] Zhang, Shaohui, Xu Di, Li Yinong, et al. An optimized inverse model used to estimate Kostikov infiltration
771 parameters and Manning's roughness coefficient based on SGA and SRFR model: I Establishment[J]. *Shuili*
772 *Xuebao*, 2006, 37(11):1297-1302.
- 773 [66] Zhang, Shaohui, Xu Di, Li Yinong, et al. Optimized inverse model used to estimate Kostikov infiltration
774 parameters and Manning's roughness coefficient based on SGA and SRFR model: II Application[J]. *Shuili*
775 *Xuebao*, 2007, 38(4):402-408.
- 776 [67] Zhang, Mengze, Liu Yuanhong, Wang Lingru, et al. Inversion on Channel Roughness for Hydrodynamic
777 Model by Using Quantum-Behaved Particle Swarm Optimization[J]. *Yellow River*, 2015, 37(2):26-29
- 778 [68] Zhao, R. J.,1977. Flood forecasting method for humid regions of China, East China College of Hydraulic
779 Engineering, Nanjing, China.